Title

THE MASS RATIO METHOD APPLIED TO THE MEASUREMENT OF L-MESON MASSES AMD THE ENERGY BALANCE IN PION DECAY

Authors

Barkas, Walter H.
Birnbaum, Wallace
Smith, Francis M.

Publication Date

1955-09-01

UCRL 3147

UNIVERSITY OF CALIFORNIA

Radiation Laboratory

BERKELEY, CALIFORNIA

DISCLAIMER

UCRL-3147

UNIVERSITY OF CALIFORNIA

Radiation Laboratory
Berkeley, California

Contract No. W-7405-eng-48

THE MASS RATIO METHOD APPLIED TO THE MEASUREMENT OF L-MESON MASSES AND THE ENERGY BALANCE IN PION DECAY

Walter H. Barkas, Wallace Birnbaum, and Frances M. Smith

September 1955

Printed for the U.S. Atomic Energy Commission

The Mass Ratio Method Applied to the Measurement of L-Meson Masses and the Energy Balance in Pion Decay

Walter H. Barkas, Wallace Birnbaum, and Frances M. Smith

Radiation Laboratory
University of California
Berkeley, California

ABSTRACT

We report a comprehensive series of measurements made on the masses of L-mesons produced by the 184-inch cyclotron. A general ratio principle of measurement is employed which largely eliminates systematic errors. The particular method that we have developed is described in detail. The theory of non-equilibrium particle orbits in the cyclotron field is worked out to provide formulas from which momenta may be calculated, and to obtain the momentum distribution functions determined by the target and detector dimensions. The energy-loss processes in nuclear track emulsion, which is used as a stopping material and detector, are studied and the range-momentum exponent q is found. Several small corrections to the mean range are made. A number of range straggling effects are evaluated. The theoretical distribution of the quantity Rp^{-q} (R being the range and p the momentum) is studied, and the first three moments of the distribution are calculated explicitly. The distribution is found to be closely gaussian. From the theory of the distribution of Rp^{-q}, the best estimate and the statistical uncertainty of the mass ratio (e.g., of meson to proton) are evaluated. A number of effects influencing the ratio are studied, but all the corrections found are very small. The measurement of the momentum acquired by the muon when a pion decays has also been treated. Several important relations connecting this quantity with the particle masses are then introduced. Apparatus developed for the application of the ratio principle is described. A number of experiments in which mesons and protons of similar velocities

were detected in the same nuclear track plate are reported. Each experiment was repeated a number of times. The measurements of particle ranges and orbit parameters, the magnetic field measurements, the dimensional tolerances, the calculations, and other important details are discussed.

The following mass ratios are reported:

$$\pi^+/\text{proton} = 0.1488_7 \pm 0.00011$$

$$\pi^-/\pi^+ = 0.998 \pm 0.002$$

$$\pi^+/\mu^+ = 1.321 \pm 0.002 .$$

The center-of-mass momentum acquired by the muon in positive pion decay was measured as 29.80 ± 0.04 Mev/c and its energy, 4.12 ± 0.02 Mev. All the results are consistent if the rest mass of the neutral particle in the pion decay is zero. With this assumption, the measurements further imply that the positive pion-muon mass difference is 66.41 ± 0.07 electron masses. The derived masses, in units of the electron mass, are:

$$\pi^+ = 273.3 \pm 0.2$$

$$\pi^- = 272.8 \pm 0.3$$

$$\mu^+ = 206.9 \pm 0.2.$$

I. INTRODUCTION

The determination of pion and muon masses presented special problems which slowed the convergence of the numerous early measurements.[1] One of the various reasons that precision is difficult to attain is that no known comparison particles with approximately the same specific charges as those of L-mesons are available, so that we cannot utilize doublets analogous to those of atomic mass spectrometry. Therefore, absolute measurements of quantities determining the mass usually were employed.

It was noticed,[2] however, that the mass normalizes a number of measurable quantities so that when divided by the mass, they become functions of the velocity alone. For particles of the same charge, the energy (total or kinetic), the momentum, the range, the total ionization, the reciprocal of the mean scattering angle, and the range variance are such quantities. For nuclear track emulsion, further quantities of this sort are obtained from the several different measures of the total amount of developed silver in the track.[3] The frequent appearance of the mass as a scale factor suggests a means for determing the ratio of the meson mass to that of a comparison particle from relative measurements. For example, if the ratio of meson momentum to proton momentum is adjusted to be equal to the ratio of the mean meson range to the mean proton range, then the velocities are equal, and the mass ratio is equal to the ratio that is common to the ranges and momenta. The same argument applies for any pair of quantities each of which can be expressed as a product of the mass and a function of the velocity.

D. H. Perkins[3] first suggested such a principle for determining ratios of meson masses from the observed numbers of developed grains in emulsion tracks as functions of the residual range. The derived mass in this example is unfortunately very sensitive to counting errors, which may be both statistical and systematic, so that the grain count and residual range are not the most

satisfactory pair of observable quantities for application of this principle. For use with existing techniques, the momentum and the range in emulsion are the most satisfactory quantities in spite of the inherent limitation set by range straggling. An important feature of our analysis is the selection for statistical treatment of a function of the measured quantities whose distribution is substantially normal, and of which the moments are calculable.

Prior to this measurement program, there had been considerable development of range and momentum methods[4] for determining particle masses, particularly by R. B. Brode and his collaborators. Because it was necessary for them to use cosmic rays, however, they did not enjoy a number of advantages that are gained when one can work with controlled particle sources in vacuum while using the strong and extensive magnetic field of the cyclotron for momentum measurements. Range plus ionization[5] measurements, and range plus scattering[6] measurements, as well as a few observations of momentum and momentum loss, momentum and electron collision, etc., have also been used to estimate meson masses.

Parallel to the application of direct means for measuring meson masses, precise indirect methods have recently been developed which invoke the conservation laws for processes in which the meson is created or destroyed or which depends on calculations of the energy states of the meson in a mesonic atom. Such methods ultimately may provide measurements of the highest precision, but it is important to insure at the outset that the phenomena themselves are fully understood. Agreement of indirect results with those obtained directly may be put forward as strong evidence for the correctness of the hypothetical reaction (and equally for the validity of the assumptions employed in the direct method). Examples of such indirect meson mass measurements are the following: (a) mass of the μ^+ meson from the end point of its positron spectrum;[7] (b) mass of the π^+ meson by analysis of its production in proton-

proton collisions;[8] (c) mass of the π^- meson from the energy of photons associated with its capture in hydrogen;[9] and (d) masses of negative mesons from energies of mesonic-atom x-ray transitions.[10]

Aside from the intrinsic importance to be attached to knowledge of the meson masses, the mass-energy balance is an obvious test of the correctness of the assumed decay process. Into the conservation equations for pion decay enter not only the masses but also the center-of-mass muon momentum. As part of this complete report we have, therefore, included measurements of this quantity in addition to mass-ratio measurements. A study has been made of the energy balance of the pion-muon decay scheme, $\pi^+ \rightarrow \mu^+ + \nu$. All the mass and kinetic-energy relations connected with the dynamics of the decay contain the mass ratio and the c.m. momentum acquired by the muon at the time of creation. This phase of the work yields a precise value for the positive pion-muon mass difference, and a new upper limit for the mass of the neutral particle ν.

II. OUTLINE OF METHOD

The principle of the mass-ratio method is sketched in this section; the detailed treatment of each phase of the analysis is taken up as a separate topic.

The theory[11] of energy loss of a charged particle penetrating matter leads to the expression

$$dT/dR = f(\beta) \ . \qquad (1)$$

This form is valid in good approximation for the mean rate of energy loss by all particles that carry the same charge and that are massive compared to the electron. In Eq. (1), $f(\beta)$ is a function of the particle velocity, R is the residual range, and T is the kinetic energy. Since T is equal to the rest mass, μ_o , times a function of the velocity, Eq. (1) can be integrated. One obtains

$$R/\mu_o = G(\beta) \ . \qquad (2)$$

A number of small corrections to Eqs. (1) and (2) are disregarded for the moment. They are treated later. Since the velocity is a function of p/μ_o, where p is the particle momentum, one can also write

$$R/\mu_o = F\,(p/\mu_o) \ . \qquad (3)$$

In our experiments, Ilford C.2 emulsion was the material in which ranges were measured. Converting the range-energy relation for protons in emulsion to a range-momentum relation, one finds that the proton data can be expressed by

$$R = c\,p^q \ . \qquad (4)$$

The exponent q is a slowly varying parameter which remains remarkably constant, with a value of about 3.44 for protons of 25 to 40 Mev.

Combining Eqs. (3) and (4), one obtains

$$R/M = c\,(p/M)^q \ , \qquad (5)$$

where M is the mass expressed in units of the proton mass.

In determining a mass ratio, one eliminates c by measuring ranges of test particles (e.g., pions) and comparison particles such as protons in the same nuclear track plate. Priming quantities associated with the comparison particle and taking its mass to be unity, one obtains the following expression for the unknown mass:

$$M^{1-q} = R/R' \, (p/p')^{-q} . \qquad (6)$$

It is important to notice that when we have the ratio $R/R' = p/p'$, a special situation exists in which M must be equal to this ratio no matter what value of q is assumed. This condition is attained when the velocity of the test particle is that of the comparison particle. In principle this equality can be approached experimentally by a method of successive approximations.[12]

In Eq. (6) only the ratios of ranges and momenta appear. Important systematic errors are eliminated by the mass-ratio method when the ranges of both types of particles are measured in the same body of stopping material and when both momenta are measured in the same magnetic field.

For the statistical treatment of the data, a function of the measured quantities is sought that is distributed almost normally and with calculable moments about the mean value. Such a quantity (see Eq. (6)) is the particle range divided by the qth power of its apparent momentum. The value of q is determined by the condition that the expectation value of the quotient not depend on the momentum in the velocity interval selected for the measurements. From the ratio of such expectation values for different particles at nearly equal velocities, one obtains a measure of the ratio of their masses which does not depend on the exponent q, on the stopping material, nor on the absolute value of the magnetic field employed to measure the momenta.

III. THE PARTICLE MOMENTUM

A. Orbit Calculations

In order to find particle masses by this method, one must measure momenta with good accuracy. The following calculations apply to all particles of charge e. The discussion, when it must be specific, relates to the situation in which the source of particles is a small target bombarded by the internal cyclotron beam, and particles emerging from the target are detected in nuclear track emulsion. One can observe the point where the particle enters the surface of the emulsion. He can also measure the angles describing the direction of particle motion at the point of detection. With the empirically known magnetic field intensity function, these data are sufficient to determine the momentum, but because the field is not uniform, the precise calculation of the momentum requires a somewhat elaborate treatment.

It is simplest to describe the particle motion in cylindrical coordinates (r, ϕ, z) coaxial with the cyclotron field (see Fig. 1). The cyclotron field is assumed for these calculations to have axial symmetry. The validity of this assumption must be verified by appropriate measurements. First one considers orbits confined to the median plane, where the magnetic field intensity is a function only of r. Then particles with small momentum describe trochoidal[13] paths reaching a minimum radius R_1 and a maximum radius R_2 (the libration limits). Let (r_1, ϕ_1) be the point of origin (the target) and (r_2, ϕ_2) the point of detection. The quantity $(r\, d\phi/dr)_2$ is also obtained from the direction of the track at the point of detection. The dynamical problem[14] is then treated by introducing the Lagrangian for the particle motion:

$$L = -\mu_0 c^2 \left[1 - \frac{\dot{r}^2 + r^2\dot{\phi}^2}{c^2}\right]^{\frac{1}{2}} + (e/c)\,\dot{\phi}\int_0^r r\,H(r)\,dr \qquad (7)$$

Now $\dot{r}^2 + r^2\dot{\phi}^2 = \beta^2 c^2$ is one constant of the motion. Since ϕ is an

ignorable coordinate, $\frac{d}{dt}\left(\frac{\partial L}{\partial \dot{\phi}}\right) = 0$, and

$$\frac{\mu_0 r^2 \dot{\phi}}{(1-\beta^2)^{1/2}} + (e/c)\int_{r_1}^{r} r H\, dr$$

is also a constant of the motion. If we define $\tan\lambda \equiv dr/rd\phi$, this constancy is expressed by

$$r\cos\lambda = r_1 \cos\lambda_1 - 1/K \int_{r_1}^{r} rHdr, \tag{8}$$

where for the momentum $\mu_0\beta\, c\, (1-\beta^2)^{-1/2}$ $\left[=(e/c)\, H\rho\right]$, we have written (e/c)K. Since the point of detection lies on the orbit, we obtain

$$K = \frac{\int_{r_1}^{r_2} r\, H\, dr}{r_1\cos\lambda_1 - r_2\cos\lambda_2} \tag{9}$$

In this expression everything is observable except λ_1.

The equation of the orbit is

$$\phi = \int_{R_1}^{r} \frac{\cot\lambda}{r}\, dr \tag{10}$$

in which λ is the function of r given by Eq. (8).

The poles in the integrand may be avoided and the integration carried out[14] by introducing a parameter γ given by

$$\cos\gamma = (R_2^2 + R_1^2 - 2r^2)/(R_2^2 - R_1^2)\ .$$

The integrated form of the orbit is

$$\phi = \arcsin\left(\frac{\rho_0 \sin\gamma}{r}\right) + a_0\gamma + \sum_{n=1}^{\infty} a_n \sin n\gamma \tag{11}$$

The a_n and ρ_0 are defined below. If the magnetic field between R_1 and R_2 is described by an even polynomial in r (that odd powers do not enter may be inferred from the behavior of the cyclotron field at r = 0) as follows,

$$\frac{H(r)-H_0}{H_0} = h_0 + h_2 r^2 + h_4 r^4 + \cdots h_{2n} r^{2n} \equiv h(r),$$

then $\int_{R_1}^{R_2} r\,h\,dr = 0$ when $H_0 \equiv \frac{2}{R_2^2 - R_1^2}\int_{R_1}^{R_2} r\,H\,dr$

Now $\rho_0 \equiv \frac{R_2 - R_1}{2}$, so $H_0\,\rho_0 = K$. We also define $R \equiv \frac{R_1 + R_2}{2}$. In terms of these quantities the a_n may be calculated. Expressions for the first three follow:

$$a_0 = \rho_0^2\left[h_2 + 2h_4(R^2+\rho_0^2) + 3h_6(R^4+3R^2\rho_0^2+\rho_0^4) - 3\rho_0^2 h_2 - h_2 h_4(7R^2\rho_0^2+6\rho_0^4) + \cdots\right]$$

$$a_1 = -R\rho_0^3\left[\tfrac{4}{3}h_4 - \tfrac{3}{2}h_2^2 + 4h_6(R^2+\rho_0^2) - (6R^2+10\rho_0^2)h_2 h_4 + \cdots\right]$$

$$a_2 = R^2\rho_0^4\left[h_6/2 - h_2 h_4 + \cdots\right]$$

The first term of Eq. (11) describes a circular orbit. The second superimposes a precession around the axis of symmetry, and the Fourier sum adds an harmonic perturbation of the precessing circular orbit. The orbit is periodically tangent to the libration circles of radii R_1 and R_2.

Equation (11) for the orbit may be used to evaluate λ_1 under arbitrary conditions; for approximately 180° bending in a slowly varying field, with $\phi_1 = \phi_2 \approx 0$, the calculation is particularly simple. In this case $\lambda_1 \approx R\,\gamma_1/r_1$; $\pi - \lambda_2 \approx R\,(\pi - \gamma_2)/r_2$; so $\lambda_1 = (\pi - \lambda_2 + \lambda_0)$, where $\lambda_0 \approx \pi/2\ \frac{H_2 - H_1}{H_2 + H_1}$. Then, from Eq. (9),

$$K = \frac{\int_{r_1}^{r_2} r\,H\,dr}{r_1\cos(\pi - \lambda_2 + \lambda_0) + r_2\cos(\pi - \lambda_2)} \qquad (12)$$

In Eq. (12) all quantities needed to determine K are measurable. A bending of 180° also enables one to measure momenta with the minimum error, as, in first approximation, the diameter of the orbit is observed directly, and the derived momentum is insensitive to the observed angle, λ_2.

To simplify the momentum calculations one introduces a rectangular coordinate frame with the x-axis lying along a radial line extending toward larger radii and with the z-axis parallel to the field axis. The origin is at the center of the target and measurements are made with apparatus constructed so that the center of the detecting plate lies along the line $z = -z_0$ in the xz plane. The angle θ', defined below, and x_0, the x coordinate at which the orbit crosses the x-axis, are then found with negligible error from the track position and direction.

For a particle starting at the center of the target,

$$K = \frac{\int_{r_1}^{r_1 + x_0} r H \, dr}{r_1 \cos(\theta' + \lambda_0) + (r_1 + x_0)\cos\theta'} \tag{13}$$

In this expression, θ' is the angle to the y-axis measured in the xy plane at which the orbit crosses the x-axis; θ' is positive when the orbit has not yet reached the outer libration limit. In our experiments, λ_0 is entirely negligible for the meson orbits but not for the proton orbits. For mesons, therefore,

$$K = \frac{\sec\theta' \int_{r_1}^{r_1 + x_0} r H \, dr}{2r_1 + x_0} \tag{13'}$$

If the angle of the orbit to the median plane (the xy plane) is γ, then $(e/c)K \sec\gamma$ is the total momentum of the particle. A nominal value of γ is $\gamma_0 \equiv \arctan \frac{2z_0}{\pi x_0}$. The quantity

$$\frac{\sec\gamma_0 \int_{r_1}^{r_1 + x_0} r H \, dr}{2r_1 + x_0}$$

may be expressed graphically as a function of x_o, so that the momentum calculations become much simplified.

Some attention must be given to the constancy of the component of particle motion perpendicular to the median plane. In our experiments this component of velocity is always small and the composition of it with the component parallel to the median plane is accomplished in multiplying eK/c by sec γ, where γ has been assumed constant along the orbit. To test the validity of this procedure, it will suffice to estimate the deviation from constancy of the velocity component perpendicular to the median plane.

If $\dot{z}_1$ is the initial component of velocity parallel to the z axis and $\Delta\dot{z}$ is the maximum change in this component, then it is readily shown that

$$\left|\Delta\dot{z}/\dot{z}_1\right| \approx (\pi/2 - 1) \quad \rho_o \, n/R,$$

where $n = -(r/H_z)\, \partial H_z/\partial r$. Here n has been assumed constant. Actually it varies slowly, but it has a maximum value in our experiments of 0.07, so even for proton orbits with $\rho_o \approx R/3$, the maximum deviation from constancy of $\dot{z}$ is not more than 1 percent. Therefore one can safely treat the two components of velocity as independent.

B. Finite-Target and Detector Effects

The apparent momentum p is calculated on the assumption that the particle starts at the center of the target and that its orbit crosses the xz plane at a definite height $(-z_o)$ with $\gamma = \gamma_o$. The target has usually been made in the form of a rectangular parallelopiped of finite dimensions 2a, 2b, and 2c in the x, y, and z directions, respectively. Furthermore, particles are accepted for measurement with θ' lying in a finite interval, and they strike the surface of the emulsion anywhere in the searched area, which is symmetrically located with respect to the x axis. Particles with a

distribution of true momentum p_1 therefore contribute to the group with apparent momentum p. Consequently, one must study the function $U(p_1,p)$, which gives the probability $U(p_1,p)dp_1$ that the true momentum lies between p_1 and $p_1 + dp_1$, when the apparent momentum is p. The question may be treated in a general manner by calculating

$$\langle p_1^n \rangle = \int p_1^n \, U(p_1,p)dp_1 = p^n (1 + \omega_n) . \qquad (14)$$

In the design of the experiments the ω_n are made as small as possible. They are evaluated as follows: With the origin at the center of the target, the orbit is assumed to begin at the point (x_1, y_1, z_1) and is observed to cross the x axis near the outer libration limit at $x = x_o$, making an angle θ' with the y axis. The emulsion surface is assumed to lie in the plane $z = -z_o - \epsilon y$ with $x_o \gg z_o$ and $\epsilon \ll 1$. The particle is observed to enter the emulsion at a point having a y coordinate equal to y_2 as illustrated in Fig. 2. The ω_n have been calculated[2g] for each experimental situation by first expanding the expression for the nth power of the momentum p_1 through terms of third order in the small quantities z_o/x_o, x_1/x_o, y_1/x_o, z_1/x_o, y_2/x_o, θ', and ϵ. Then the appropriate mean values are introduced.

The distributions of θ' and y_2 are observed. The distributions of x_1, y_1, and z_1 can be inferred from the geometry of the target and other information relating to the problem. For μ^+ mesons coming from the target,[2i] all the particles are assumed to arise from the decay of π^+ mesons that stop in a very thin layer on the surface of the target. Because the only muons accepted for measurement are those which have nearly the characteristic decay velocity, such particles could not have emerged from deep in the target. No negative values of θ' can be associated with muons coming from the surface $x = +a$, and no positive values of θ' are associated with muons coming from the surface $x = -a$. One actually observes a number N^+ with θ' positive and N^- with θ' negative. For protons and pions it is assumed that

the orbits start with equal probability anywhere in the target. This is a justified assumption because on the one hand measurements of the radioactivity throughout the target show the activity to be uniform, and on the other hand the nature of the low-energy pion spectrum is fairly well described by stating that the number of mesons per unit range interval is approximately constant. The energy loss in the target, then, has little effect on the distribution of positions from which the mesons come. In all cases the finite-target effects are small, and for the protons, as will be shown, they are almost completely negligible.

IV. THE PARTICLE RANGE

A. Energy-Loss Processes

Three effects contribute to the average rate of energy loss of a charged particle penetrating matter. For our experiments they are, in ascending importance, (a) radiation loss, (b) energy loss to nuclei, and (c) energy loss to electrons. We must examine these processes in sufficient detail[2g] that we may make appropriate corrections where necessary to the basic Eqs. (1) and (2).

1. Energy Loss by Radiation

The initial velocity was selected to be about 0.27 c. For such a velocity the total energy loss by radiation is about 1.5×10^{-5} Mev irrespective of mass.[15] It is an entirely negligible part of the total energy lost in coming to rest.

2. Energy Loss in Nuclear Collisions

The energy loss in nuclear collisions[2g] is about (M/100) Mev (M being the mass in units of the proton mass). This does not alter the form of Eq. (1), and the whole effect is small in any case, so no special allowance for the energy loss to nuclei is required.

3. Energy Loss to Electrons

Interaction with electrons is the predominant energy-loss process for fast charged particles penetrating emulsion, and here the Bethe-Bloch theory[11,16] expresses the rate of energy loss quite well. At low velocities no known analytic expression is strictly correct. The initial particle velocity chosen by us is higher than that of any of the stopping electrons except the K electrons of Br, Ag, and I. Consequently, the theory has reasonable validity. However, one of the fundamental advances made in this method of mass measurement is an avoidance of any real dependence on the nature of the stopping material or on a detailed theory of stopping. The

existence of an explicit stopping formula is more a convenience than a necessity.

For a composite material such as emulsion, the usual theoretical expression for the mean rate of energy loss of a fast particle to electrons becomes

$$-\left\langle \frac{dT}{dx} \right\rangle = \frac{4\pi}{\beta^2}\left(\frac{e^2}{mc^2}\right)^2 \sum_i (N_i Z_i) \ln \frac{2mc^2}{J} \frac{1}{\left(1+\frac{m}{\mu}\right)^2} \frac{\beta^2 e^{-\beta^2}}{(1-\beta^2)} \quad mc^2/cm \quad (15)$$

In this expression J is defined by

$$\ln J = \frac{\sum_i N_i Z_i \ln J_i}{\sum_i N_i Z_i}$$

where J_i is the appropriate mean ionization potential of the ith type of atom in the emulsion. J_i/Z_i is a slowly varying function of Z. Using the data of Bakker and Segre[17], we determined J_i graphically for each element in the emulsion from the curve of J_i/Z_i vs Z_i. Assuming the stated composition of Ilford C.2 emulsion, we found J to be 270 ev.

B. Sign Dependence of Stopping Cross Section

In a preliminary report we called attention[2f] to the possible difference in stopping cross sections for particles of opposite sign. The late Professor Enrico Fermi[18] has provided us with an estimate of this difference. The result of his calculation is to raise the apparent mass of the negative pion in our experiments by 9 parts in 10^4. We make this correction in the final results quoted in this paper.

C. Determination of the Momentum Exponent

Suppose protons of momentum p_i have a mean range R_i. Then we may write the momentum-range relation in the vicinity of the point (p_i, R_i) as $R/R_i = (p/p_i)^{q_i}$, and, regarding q as a function of β,

$$q = p/R\left(\frac{dR}{dp}\right) = \frac{\beta^2}{(1-\beta^2)^{\frac{1}{2}}(dT/dR)\int_0^{\beta}\frac{\beta\,d\beta}{(1-\beta^2)^{3/2}(dT/dR)}} \quad (16)$$

The quantity $dT/dR = -\left\langle\frac{dT}{dx}\right\rangle$ depends on β, J, and the effective density n_e of electrons. One or both of the quantities n_e and J must be regarded as a function of β when βc is comparable to the velocity of any of the emulsion electrons. A semiempirical evaluation of the energy loss function in emulsion has been made by Vigneron.[16] He states that the value of J must be taken considerably higher than that implied by the data of Bakker and Segre. He extrapolated the proton range curve to energies beyond the accurate measurements known to him, using a value of J = 332 (±25) ev. in the high-energy region. His calculations predict precisely the proton range (4580 ± 18 microns) at 33.64 Mev observed incidentally to the mass measurements reported here. At higher velocities, however, the measurements by Otto Heinz[19] favor a mean ionization potential of 276 ± 28 ev. The behavior of q when J = 270 ev is used in Eq. (15) is compared with q as determined from Vigneron's data for protons in Table I.

Table I

Computed Values of q

T (Mev)	10	15	20	25	30	35	40	45
q_{270}	3.36	3.40	3.43	3.444	3.447	3.446	3.440	3.43
$q_{Vig.}$	3.41	3.44	3.460	3.465	3.465	3.461	3.456	3.45

The stability of q is remarkable. The slope, dq/dT, passes through zero in the vicinity of the velocity interval employed for the mass measurements. In this region q depends only on J and is very insensitive to it. The mass calculations were actually carried out using q = 3.44 from an earlier estimate.[2e] Because the derived mass is insensitive to the value of q

employed, it makes no difference in the results obtained whether 3.44 or 3.46 is adopted for the value of q. Since the Vigneron value of q and that obtained on assuming a value of J = 270 ev are near the limits within which q may reasonably lie, an estimated error of 0.03 in q is adequate.

D. Range Straggling

The particle mass and momentum are connected through Eq. (5) with the mean range of the particle. Our experiments measure the distribution of a random variable, Rp^{-q} (the normalized range), and the particle mass ratios are calculated from the observed mean values of such quantities. For the mass calculation to be trustworthy, however, it is necessary that one be able to account for all the significant contributions to the variance of Rp^{-q}. In particular, it is important that the measured particles originate only at the target. Using our theoretical distributions of R and p, we are in a position to compare the expected distribution of the normalized range with that observed. In this way, contamination of the mesons with particles that could not have come from the target has been detected in the distribution of Rp^{-q} observed in an earlier experiment.[2c] The background mesons had the effect of raising the apparent mass by an amount that exceeded the statistical probable error of the measurements. Our present results, however, are understandable in terms of the known sources of variance. This is a satisfactory situation for the reliability of the data, and it is submitted also as evidence that the mass values are discrete.

A charged particle is brought to rest in matter by numerous collisions, chiefly with electrons. The number of these interactions per unit path and the amount of energy lost in each collision are governed by chance, so that the distances traveled by individual particles of a monoenergetic group in coming to rest will vary. The fact that emulsion is not a rigid homogeneous stopping material complicates this behavior, so that

for a full understanding of the range straggling in emulsion, we carried out a supplementary investigation.[20] The contributions to the variance of Rp^{-q} in a typical plate (No. 28849) are quoted briefly in Table II. The total variance anticipated is found by calculating the sum of the squares of the separate straggling effects, each of which is discussed in Reference 20. In our experiments, the emulsion distortion was measured in most of the plates. It seldom introduced an important contribution to the straggling.

Table II

Percentage standard deviation of Rp^{-q} for positive muons, positive pions, and protons at $\beta \approx 0.27$ in plate No. 28849. Data quoted from Reference 20.

Particle	Bohr straggling	Proportional straggling	Macroscopic distortion straggling	Momentum straggling	Calculated straggling	Observed straggling
μ^+	4.0	1.0	1.3	0.0	4.3	4.6 ± 0.4
π^+	3.5	0.9	0.2	0.7	3.7	3.7 ± 0.4
proton	1.35	0.36	0.16	0.24	1.42	1.5 ± 0.3

Where a distortion effect was detected in the mean range, corrections were made to the final mass values. (See Section VIII.)

As pointed out by Lewis[21], the mean range is not given exactly by Eq. (2), but the right side of the equation is slightly dependent on the mass. The range is increased[20,21] by the factor $1 + e_1$, where $e_1 \approx 0.41/T\langle dT/dR\rangle$. In this expression e_1 is dimensionless, T is in Mev, and R in cm. This effect, which is closely related to the range straggling, has been evaluated and the appropriate correction (which is very small) made in the mass calculation (Section VIII). For a particle whose mass is very large compared to that of an electron we write Eq. (5) in the form

$$R/M = c_o (p/M)^{q_o} .$$

Then q and q_o will differ by $\approx p_1 \frac{de_1}{dp_1}$. In our experiments this is only about 10^{-4} for mesons, so that correction of q for this effect is trivial.

A statistical effect extending the mean range, similar to the Lewis Effect, arises from the heterogeneity of the emulsion. This range extension has also been estimated. It is a very small fraction of the range when the range is large, only about 0.1 micron. It has been neglected. On the other hand, a correction of 0.9 micron has been made for the finite grain-spacing effect.[20]

A further effect on the mean range and on the apparent range straggling is introduced if the factor by which the emulsion shrinks in processing is incorrectly estimated. If S_o is the correct shrinkage factor and the shrinkage factor assumed is S, then we symbolize the error in the shrinkage factor by $\Delta S = S - S_o$. From an independent series of experiments[22] we take $S = 2.3$, and for its uncertainty we estimate $\Delta S^2 = \sigma_S^2 = 0.01$.

These effects, which influence the mean range, lead us to distinguish between the ideal quantity R of Eq. (2) and the actual measured range R_1.

V. STATISTICAL CALCULATION OF MASS RATIOS

Equation (6) provides the basic formula for the calculation of the mass of a particle in units of the mass of a comparison particle. Measurements on a single meson track when compared with similar data from the track of another particle yield an estimate of their mass ratio, but because of range straggling, the finite target size, and the finite area of detector that must be scanned, the measurement of particle masses can be made with much higher precision if one understands the distribution of the quantity $R_1 p^{-q}$. The empirical distribution function is found, of course, by measuring the track length R_1 and the apparent momentum p for many particles.

If we use the average value of the observed quantity $R_1 p^{-q}$ instead of Rp^{-q} in Eq. (6), it leads to an apparent mass ratio M_1, defined by

$$M_1^{1-q} = \langle R_1 p^{-q} \rangle \Big/ \langle R_1' p'^{-q} \rangle \quad , \tag{17}$$

where again the prime refers to the comparison particle. The connection between M_1 and the true mass ratio M can be obtained by utilizing the information we possess regarding the various distribution functions.

As in Section III, let $U(p_1,p)dp_1$ be the probability that the true momentum lies between p_1 and $p_1 + dp_1$ when the apparent momentum is p. Also let $V(R_1,p_1)dR_1$ be the probability that the observed track length will lie between R_1 and $R_1 + dR_1$ when the momentum is p_1, and let $W(p)dp$ be the fraction of the measured values of the apparent momentum which lies between p and $p + dp$. Then the nth moment of the distribution of $R_1 p^{-q}$ may be calculated:

$$\langle R_1^{\,n} p^{-nq} \rangle = \int_p \int_{p_1} \int_{R_1} R_1^{\,n} p^{-nq} W(p)\, U(p_1,p)\, V(R_1,p_1)\, dp\, dp_1\, dR_1 \tag{18}$$

For carrying out the integrations we define

$$\langle p \rangle = \int pW(p)dp \text{ and } \sigma_p^2 = \int (p - \langle p \rangle)^2 W(p)dp.$$

Both these quantities are obtained from the observed distribution of p. In our experiments $\sigma_p \ll \langle p \rangle$. We also note that the sign of the error in q is unknown, so $\langle q - q_o \rangle = 0$. For the same reason we take $\langle S - S_o \rangle = 0$. We describe the uncertainty in q by an estimated standard deviation σ_q, and in S by σ_S.

Then from Eq. (18) we obtain several quantities of interest:

(a) The mean value of $R_1 p^{-q}$,

$$\langle R_1 p^{-q} \rangle = c_o M^{1-q} (1 + e_1 + \omega_q), \tag{19}$$

where ω_q and e_1 have been defined above;

(b) The variance σ^2 of $R_1 p^{-q}$,

$$\sigma^2 = \langle R_1^2 p^{-2q} \rangle - \langle R_1 p^{-q} \rangle^2 = \langle p \rangle^{-2q} \left[\sigma_R^2 + \langle R_1 \rangle^2 (\omega_{2q} - 2\omega_q) \right] \tag{20}$$

(c) The asymmetry Δ^3 of $R_1 p^{-q}$,

$$\Delta^3 = \langle R_1^3 p^{-3q} \rangle - 3\langle R_1 p^{-q} \rangle \langle R_1^2 p^{-2q} \rangle + 2\langle R_1 p^{-q} \rangle^3$$

or

$$\Delta^3 = \langle p \rangle^{-3q} \left[\beta_3 + \langle R_1 \rangle^3 (\omega_{3q} - 3\omega_{2q} + 3\omega_q + \frac{3q(2q+1)\sigma_p^2 \sigma_R^2}{\langle p \rangle^2 \langle R_1 \rangle^2}) \right] \tag{21}$$

We then obtain for the mass, M:

$$M = M_1 \left[1 + \frac{e_1 - e_1'}{q-1} + \frac{\omega_q - \omega_q'}{q-1} \right] \tag{22}$$

If there are n observations of $R_1 p^{-q}$ and n' observations of $R_1' p'^{-q}$, the variance σ_M^2 of this calculated mass is

$$\sigma_M^2 = \frac{M^2}{(q-1)^2}\left\{\frac{\sigma^2}{n\langle R_1 p^{-q}\rangle^2} + \frac{\sigma'^2}{n'\langle R_1' p'^{-q}\rangle^2}\right.$$

$$+ \frac{\sigma_q^2}{4}\left(\frac{\sigma_p^2}{\langle p\rangle^2} - \frac{\sigma_{p'}^2}{\langle p'\rangle^2} - 2r\right) \qquad (23)$$

$$\left. + \frac{\sigma_s^2}{s^2}\left(\langle \sin^2\delta\rangle - \langle \sin^2\delta'\rangle\right)^2\right\},$$

where $\langle p\rangle / \langle p'\rangle \equiv M(1+r)$ and δ and δ' are the respective dip angles in the emulsion of the measured tracks as defined in Reference 20.

Since the observed distributions of θ' and y_2 are employed in calculating the mass variance, it would be incorrect to make a further statistical allowance for observational errors in these measurements.

Errors in determining the linear dimensions of the apparatus and the shape of the magnetic field distribution have not been included in Eq. (31). The experiments were designed so that these effects would not be large enough to affect the results by more than a few parts in ten thousand.

We have assumed that the absolute magnitude of the electric charge of the various kinds of mesons is the same as that of the proton, and it has also been assumed that the stopping is solely an electromagnetic effect. Should these assumptions be inexact, this inexactness may be revealed by discrepancies between the results reported here and precise measurements made by other means.

To obtain the pion mass in units of the muon mass, a ratio which we call α, one uses the equations above with the muon as the comparison particle. The groups of particles are measured in the same plate, and their

momentum intervals are selected so that the ratio of their momenta is close to a. The ratio of the negative pion mass to that of the positive pion is found in an analogous manner. Although in these experiments the proton mass is usually taken as unity and the fundamental positive pion/proton mass ratio is measured, it is a matter of convention eventually to express all results in electron mass units.

VI. ANALYSIS OF PION DECAY

A. Relations Derived from Conservation Laws

A careful study of the energy and momentum balance of the assumed mode of pion decay not only tests the validity of the assumption, but also yields accurate meson-mass relations in terms of observable quantities. The pion, π, is supposed to decay into a muon, μ, and a neutral particle, ν, usually assumed to be a neutrino. The process of decay requires the sudden creation of a high-velocity muon which must be accompanied by a continuous photon spectrum. Therefore, kinetic energies of the muon from zero to the full energy T_o are possible. Several authors[23] have obtained expressions for the distribution function $P(T,W)dTdW$, for the probability that the muon energy will lie in the interval dT and be accompanied by a photon with energy in the interval dW. If one integrates $P(T,W)dTdW$ with respect to W, he obtains the probability $Q(T)dT$ that the muon possesses a kinetic energy lying between T and T + dT. The ratio of the probability of soft-photon decay to radiationless decay for $T < 3.5$ Mev is calculated to be ≈ 1.3 to 2.0×10^{-4}. Fry[24], examining anomalously short muon tracks which cannot be explained by decay in flight, has obtained an experimental value for this probability of $(3.3 \pm 1.6) \times 10^{-4}$, which is in agreement as to order of magnitude. In any event, the probability of obtaining a "low-energy" μ meson is very small. If one calculates the mean energy of the muon, allowing for the presence of the complete bremsstrahlung spectrum, it is found to be but a few hundred electron volts less than the radiationless value of ≈ 4.1 Mev. Since no anomalously short-range tracks are included in the analysis given here, the effect of the inner bremsstrahlung process is felt even less and is too small to be detected in our experiments. Therefore, the decay of the pion may be treated as a simple two-body problem. We write the relativistic equations for the conservation of energy and momentum for a pion

decaying while at rest as follows:

$$m_\pi c^2 = (p_o^2c^2 + m_\mu^2c^4)^{1/2} + (p_\nu^2c^2 + m_\nu^2c^4)^{1/2} = m_\mu c^2 + T_\mu + m_\nu c^2 + T_\nu, \quad (24a)$$

$$p_o = p_\nu \, . \quad (24b)$$

For clarity we distinguish between the momentum p_μ of a μ meson coming from the target and entering the emulsion, and the momentum p_o of the μ meson acquired at the instant of its creation.

From Eq. (24),

$$m_\nu = m_\mu \left[a^2 + 1 - 2a \sqrt{1 + (p_o/m_\mu c)^2} \right]^{1/2} \, . \quad (25)$$

with $a \equiv m_\pi/m_\mu$.

One cannot hope by measuring a, m_μ, and p_o to obtain a value for the rest mass of the presumed neutrino with an accuracy comparable to that obtained in beta-decay studies, because, as shown in Eq. (25), the mass of the neutral particle is obtained from the difference of two comparatively large numbers. One can merely derive a new limit for the mass of the neutral particle and decide if there are any inconsistencies in the presumed mode of decay.

On the other hand, certain quantities can be obtained which are very insensitive to the mass of the neutral particle if it is indeed quite small. Hence, assuming $m_\nu = 0$, we have several important relations as follows:

1. The Pion-Muon Mass Difference:

$$m_\pi - m_\mu = \frac{2a}{a + 1} \, p_o/c \, . \quad (26)$$

As is shown later, very good accuracy can be obtained in the estimate of the mass difference. This difference, coupled with the value of the mass ratio a enables one to derive absolute values of the positive pion and muon masses, independent of any other comparison particle such as the proton.

2. Masses of the Muon and Pion:

$$m_\pi = a m_\mu = \frac{2a^2}{a^2 - 1} \; p_o/c \; . \tag{27}$$

3. Kinetic Energy of the Muon:

$$T_o = \frac{a - 1}{a + 1} \; p_o c = \frac{(a - 1)^2}{2a} \; m_\mu c^2 \tag{28}$$

From the usual relativistic relations, one can also write the kinetic energy with no assumptions regarding the mass of the neutral particle,

$$T_o = (p_o^2 c^2 + m_\mu^2 c^4)^{1/2} - m_\mu c^2 \; . \tag{29}$$

B. The Absolute Muon Decay Momentum

The conservation relations for the decay process involve the mass ratio a and the decay momentum p_o. The details of determining a have been discussed, and we now concern ourselves with the evaluation of the other important parameter, p_o.

The μ mesons entering the detector from the target come from the decay of pions that stop in the target. They no longer have their full decay energy, owing to energy losses within the target. The ranges of μ mesons created within the emulsion itself, however, also are measured. These mesons are referred to as "μ-completes" with momentum p_o, while the muons coming from the target we term "ρ mesons" with momentum p_μ.

Two methods involving the fundamental Eq. (6) are employed to determine p_o. In the first method, the μ-completes are compared with the ρ mesons. Then the masses are the same. In Eq. (6) let $p = p_o$ and $p' = p_\mu$, with associated residual ranges R_o and R_μ, respectively. Solving for the absolute decay momentum, we get

$$p_o = \left[\frac{R_o}{R_\mu p_\mu^{-q}} \right]^{1/q} \tag{30}$$

Now, however, the determination of an absolute value for p_o requires an

absolute measurement of the magnetic field of the cyclotron. The velocities of the two sets of mesons are to be chosen as nearly equal as is consistent with having adequate statistics for the analysis. This is desirable, once again, to insure that the uncertainty in q not be a significant source of error. Using the mean range of the μ-completes as well as the mean value of the normalized range, $R_{1\mu}p_{\mu}^{-q}$, and introducing the various corrections, one obtains

$$p_0 = \left[\frac{\langle R_0\rangle}{\langle R_{1\mu}\, p_{\mu}^{-q}\rangle}\right]^{\frac{1}{q}}\left[1 + \frac{e_{1\mu} - e_{10}}{q} + \frac{\omega_{q\mu}}{q}\right] \qquad (31)$$

The subscripts o and μ identify the groups of muons to which the symbols refer.

If we define t by the relation $t \equiv \frac{\langle p_\mu\rangle - p_0}{p_0}$, where p_μ is the mean momentum of the ρ mesons that are selected for range measurements, the uncertainty in p_0 may be expressed by

$$\frac{\sigma_{p_0}^2}{p_0^2} = \frac{1}{q^2}\left\{\frac{\sigma_{R_0}^2}{n_0\langle R_0\rangle^2} + \frac{\sigma_\mu^2}{n_\mu\langle R_{1\mu}\, p_\mu^{-q}\rangle} + \frac{\sigma_q^2}{4}\left(\frac{\sigma_{p_\mu}^2}{\langle p_\mu\rangle^2} + 2t\right)\right. \qquad (32)$$

$$\left. + \frac{\sigma_\delta^2}{\delta^2}\left[\langle \sin^2\delta_\mu\rangle - \langle \sin^2\delta_0\rangle\right]^2\right\} + \frac{\sigma_H^2}{H^2}$$

where $\sigma_{R_0}^2$ is the observed variance or range straggling of n_0 μ-complete events. The additional term, $\frac{\sigma_{H^2}}{H^2}$, represents the uncertainty in the magnitude of the absolute value of the magnetic field.

In the second method, the mean range and momentum of the μ-completes are compared with the ranges and absolute momenta of π mesons originating at the target and entering the emulsion detector. Again the velocities of the two particles are to be chosen approximately equal. Applying the fundamental

Eq. (6), we solve for p_o, obtaining

$$p_o = \left[\frac{\langle R_o \rangle}{\alpha^{q-1}\langle R_{1\pi} p_\pi^{-q}\rangle}\right]^{\frac{1}{q}}\left[1 + \frac{e_{1\pi} - e_{1o}}{q} + \frac{\omega_{q\pi}}{q}\right] \qquad (33)$$

Thus, knowing the value of the mass ratio α from an independent study, we have another method for evaluating the absolute decay momentum of the muon. If we take $\langle p_\pi \rangle / p_o \equiv \alpha(1 \pm s)$, we now express the uncertainty in p_o as follows:

$$\frac{\sigma_{p_o}^2}{p_o^2} = \frac{1}{q^2}\left\{\frac{\sigma_{R_o}^2}{n_o\langle R_o\rangle^2} + \frac{\sigma_\pi^2}{n_\pi\langle R_{1\pi} p_\pi^{-q}\rangle^2}\right. \qquad (34)$$

$$+ (1-q)^2\frac{\sigma_\alpha^2}{\alpha^2} + \frac{\sigma_q^2}{4}\left(\frac{\sigma_{p_\pi}^2}{\langle p_\pi\rangle^2} + 2\rho\right)^2$$

$$\left. + \frac{\sigma_s^2}{s^2}\left[\langle \sin^2\delta_\pi\rangle - \langle \sin^2\delta_o\rangle\right]^2\right\} + \frac{\sigma_H^2}{H^2}$$

where σ_a^2 measures the uncertainty in the value of the π/μ mass ratio.

VII. EXPERIMENTS PERFORMED

A. General Description

Only the three final experiments of an extended mass measurement program are described in this paper. These were made with the 184-inch cyclotron. The program was directed specifically to measurements of particle mass ratios and the muon decay momentum. These experiments made use of apparatus and techniques developed in a long series of earlier experiments. The measured quantities are so interrelated that, taken together, the experiments provided rather complete information on the meson masses and the energy balance in positive pion decay. Some of the quantities were actually overdetermined in the process. It should be understood, however, that the negative muon mass was not measured, nor was the decay of the negative pion studied.

Experiment 1. In this experiment positive and negative pions and protons, all in the same velocity interval, were simultaneously detected in a single nuclear track plate. The experiment was carried out three times, yielding data on plates numbered 27152, 27153, and 27154. The information obtained enables one to calculate π^+/proton and π^-/π^+ mass ratios.

Experiment 2. In this experiment conditions were made favorable for comparing the masses of the positive pion and proton, but negative pions were not detected. The center-of-mass momentum of the muon, p_o, was also measured by utilizing the measured π^+/μ^+ ratio from Experiment 3, along with the muon range R_o and the pion normalized range. Experiment 2 was carried out three times, yielding plates numbered 28848, 28849, and 28853.

Experiment 3. The π^+/μ^+ mass ratio, a, was determined by using pions and muons coming simultaneously from a single target to the detecting plate. By measuring pions of appropriately greater momentum, we obtained data for the two kinds of mesons at the same velocity. Also, by comparison of the ranges of muons created by the decay of pions in the emulsion with the ranges of

muons coming from the target with measurable momentum, the characteristic decay momentum p_o was determined. This experiment was repeated five times, yielding data from plates numbered 25957, 25958, 25959, 25961, and 25967.

The detector used in all these measurements was 1-by-3-inch glass-backed nuclear track emulsion; Ilford C.2 emulsion 200 microns in thickness was chosen because its sensitivity was sufficient to detect the particles whose tracks were to be measured, and a greater thickness would have led to more error from the distortion and shrinkage effects. Emulsion is well suited to these measurements as it performs the functions of both absorber and detector. It provides visual evidence of the progress of the particle and thus allows an accurate determination of the total range. The fairly high stopping power permits absorption of particles of moderate energy within a relatively short distance. The different kinds of particles were rather easily recognized by their appearance in emulsion. Thus, each π^+ meson was seen to decay into a muon on stopping, and for a particle to be accepted for measurement as a π^- meson, it was required to make a star.

The magnetic field intensity of the 184-inch cyclotron decreases gradually and nearly linearly from a nominal value of 15,000 gauss at the center to 94.6% of this value at a radius of 80 inches. Therefore, all particle orbits except the equilibrium orbits precess about the center of the cyclotron. The small orbits followed by particles in these experiments are trochoidal (see Fig. 1). Vertical oscillations also are present, and the median surface at which the radial component of the field vanishes is not precisely a plane, so that the level of the circulating proton beam varies as it expands radially. The beam loses stability at a radius of 81 inches and targets are not placed beyond this point.

To take full advantage of the ratio principle, it was necessary that the particles be compared approximately at the same velocity. Since the

velocity acquired by the muon when the pion decays at rest is fixed, all other particle velocities were matched to it, thus determining the apparatus dimensions. The velocity differences were small enough so that the uncertainty in q contributed only a negligible amount to the uncertainty of the mass ratios or to the absolute momentum measurement.

All the experiments were carried out in darkness, as it was necessary that the plates be exposed without any wrapping. Light from arcs to the dee and light emanating from the hot cathode of the ion source caused trouble. The apparatus was designed, therefore, so as to shield the plates from light as well as from stray protons and neutrons. The curved channels in the shielding through which the particles to be measured reached the plates were blackened on the inside.

B. Apparatus Details

In order that the protons and mesons could all experience 180° focusing and reach a single plate at the same velocity, it was necessary to provide separate targets as sources for protons and mesons. The arrangement is shown schematically in Fig. 3 and in somewhat more detail in Fig. 4. This apparatus was employed for both Experiment 1 and Experiment 2. The difference between the apparatus for these experiments was chiefly in the construction of the plate holder and in the replacement of the negative channel of Experiment 1 by copper shielding in Experiment 2.

The particles, having left the target in a fairly flat downward-spiraling trajectory, entered the surface of the emulsion with a slight dip angle (which we called δ). The target-detector assembly was so constructed that a straight line from the center of the cyclotron passed through the centers of both targets and along the long axis of the plate. We called this the Central Radial Line. For purposes of reference and calculation a local

rectangular coordinate system was adopted with the x axis extending from the target along the Central Radial Line. In the calculation of the momentum, it should be emphasized that the locations of the target and detector are considered with reference to two coordinate systems. The local reference frame has its origin at the center of the target. In this frame, the distance between the target and detector is known to high accuracy ($\approx$ 1 part in 10^4), and the entire target-detector assembly remains fixed on its base for a particular exposure. The error in the target-to-detector distance introduces an equal percentage uncertainty in the momentum. The second frame of reference has its origin at the center of the cyclotron, for the absolute value of the magnetic field was measured as a function of the cyclotron radius. The proton probe cart carrying the target-detector assembly can be set at any desired radius to an accuracy of $\approx$ 1/8 inch. Since the inhomogeneity of the field in this region is about 10 gausses per inch, the error in the location of the cart gives an error in the momentum about one part in 10^4.

Limitations of space and considerations of background made it advisable to receive pions and protons on different parts of the plate. Consequently, after exposure to protons the proton target was removed and the entire assembly was moved two inches farther away from the center of the cyclotron so that the pions also would be received at 80 inches. This was chosen as the radius for reception of the particles in order to obtain the highest bombardment energy on the targets and yet confine the orbits to the region where the field varies slowly.

The apparatus was carefully designed to avoid contamination by pions not from the target and by those that scattered from the channel walls. The pion channels were built of copper around a central orbit 7 inches in diameter. The channels admitted orbits having angles up to $\pm$ 10° with respect to the local y axis. The channels were designed so that particles scattered from

their walls could not enter the emulsion at an acceptable entrance angle and still lie near the chosen velocity interval. The proton channel was built around a central orbit 46.6 inches in diameter. The channel aperture allowed entry of orbits emitted within 2° of the y axis. The walls of these copper channels were lined with polyethylene, with the idea that the scattering of particles hitting the walls would be reduced. The channel assembly including the two targets and the nuclear track plate constituted the particle camera.

The camera was built on a cart mounted on rails affixed to the end of a radial probe extending into the cyclotron vacuum chamber. The probe was a cylindrical shaft of brass which passed into an air lock through a vacuum seal in the door. When the air-lock door had been clamped into place and vacuum had been established, the door to the vacuum chamber was opened and the whole apparatus was inserted into the cyclotron. Because the dimensions of the necessary proton orbit were greater than those of the air lock, the proton target was mounted on an extensible rod which was retracted while the equipment was in the air lock. When the cart was moved toward the center of the vacuum chamber, the rod was extended (by means of a length of strong vacuum-hose rubber under tension) until it was brought up against a positive stop when the target was the proper distance from the plate.

The target in which pions were produced (see Fig. 5) consisted of a small block of copper of width $2a = 0.044$ inch, length $2b = 0.238$ inch, and height $2c = 0.361$ inch. The width was parallel to the Central Radial Line and the length was parallel to the bombarding proton beam. The holder was a thin 8-inch bar of brass with 1.25-inch arms projecting at each end. The target was suspended between the ends of these arms by means of 0.001-inch tungsten wire, which was under tension to keep the copper target in place. No orbits from the body of the target holder could terminate on the plate; no

particles from the bottom of the channel could enter the surface of the emulsion; any particle that scattered from the top of the channel and entered the emulsion would have too large a dip angle to be accepted. The proton target was an 8-inch cylinder of 0.125-inch tungsten, fitted tightly into a vertical hole on the end of the extensible rod (see Fig. 4). It was firmly seated by means of a setscrew which clamped it into position. The effective height 2c of the target was obtained from the vertical spread of radioactivity over the cylinder after bombardment. The activity was found to be strong over a distance of 1.5 inches. Therefore c = 0.75 inch. The distribution of the bombarding beam must also be considered in pion production. There is a possibility of pion emission from the 0.001-inch tungsten wires that suspend the pion target. Consideration of the volumes involved, however, leads one to expect only one pion from the wire for every 1,000 from the target. In addition, a mock pion target, consisting of four 10-mil copper pieces pressed together, was bombarded to check the radial distribution of the beam on the target. Each section when separated showed essentially the same induced radioactivity.

The plate holder, designed for Experiment 1, was altered slightly to provide for a tilt of the plate in Experiment 2. It was made from a brass block 1 by 3 by 3/8 inches. Attached to the top edges were three small phospher-bronze leaf springs, which served to align the detector plate with respect to the top of the holder as well as to clamp it tightly in place.

Experiment 1. Both positive and negative pions were to be detected; therefore, the top of the plate holder was in a horizontal plane. The height of the plate holder was governed by our choice of about 7° for the pitch angle γ_o of the central orbits originating from the center of the target. The center of the pion target was a distance z_o of 1.36 inches above the plane of the emulsion. The corresponding distance for the protons, however, was 0.61 inch (owing to the radial variation of the beam level). Thus γ_o

for the protons was about 0.5°. Accepted angles θ' were from -10° to 10° for mesons and -2° to 2° for protons.

Experiment 2. In this experiment positive pions and protons were observed. The pitch angle of the central orbits was reduced in order to reduce the error in the momentum arising from the uncertainty in its vertical component. This was accomplished by raising the channel assembly (with the plate holder) 0.38 inch. However, we wanted the pions to have about the same angle of dip as before. Therefore a 2° slant toward the positive channels was put in the top of the plate holder. The height z_o for pions was 0.98 inch and for protons 0.23 inch.

The positions of the targets with respect to the entrance points of the particles were established by means of fiducial marks photographed directly on the emulsion. This was accomplished with a slit system built into the plate holder. The system consisted of two cross-shaped slits spaced 2 inches apart with the center of each 0.5 inch from the edges and the adjacent end of the plate. The arms of the slits were aligned with the Central Radial Line to better than 0.2° on a milling machine. Behind each of these slits was a small flashlight bulb. The bulbs were lighted for a few seconds after the detector plate was mounted (emulsion up) on the plate holder. A latent image of the slits was thereby left on the bottom surface of the emulsion. These lines not only give a permanent record of the exact position of the detector at the time of exposure, but also enable the investigator to locate quickly the proper regions of the plate to be scanned under the microscope (i.e., momentum intervals that give approximately equal velocities for the various particles). In Experiment 2 the accepted angular interval of θ' was the same as in Experiment 1.

The distances from the targets to the respective fiducial slits were measured with respect to lines inscribed on a long brass measuring bar. The

Positive pions leaving the target with energies acceptable to the defining channel spiral down under the influence of the cyclotron magnetic field and enter the detecting emulsion. Because of the channel width, the points of entry of the pions are distributed more or less uniformly over the entire plate. The positive pions that come to rest within the target decay into muons. The muons created near the surface of the target leave with only small energy losses and can be accepted by the channel, but since their momentum does not exceed p_0, they enter the emulsion in a more limited region of the plate. The pions reaching the detecting plate stop within the emulsion, giving rise to muons, approximately 17 percent of which come to the ends of their ranges before leaving the emulsion.

Previous estimates of the π/μ mass ratio indicated a value of about 1.3. In order to apply the equal-velocity principle, we therefore chose the orbit diameters in this ratio.

As described previously, the channels were so designed that any meson that scattered from the wall would either enter the detector with the wrong angle or would have a considerably lower or higher energy. Such mesons were separable from the main distribution by the range measurement. This is illustrated by Fig. 7, which shows the distributions of the normalized ranges of the mesons measured on a typical plate. A certain amount of decay in flight occurs that cannot be prevented from reaching the detector. In contrast to Experiment 3, no background mesons were found in Experiments 1 and 2.

The detecting plate was mounted on a 1-by-3-inch plate holder having an inclination angle of 5° with respect to the horizontal x-y plane. It was similar to those used in Experiments 1 and 2, and the fiducial marking was carried out in the same way. Accepted angles θ' were -11° to 11° for pions, and -15° to 11° for ρ mesons.

C. Exposures

The exposures consisted of bombarding the various targets for 30 to 45 seconds with a circulating proton beam of about 10^{-7} ampere. The beam energy at the proton target was about 70 Mev and at the meson target about 230 Mev. During exposure to pions in Experiments 1 and 2 the proton channel was plugged to reduce background. Since the emission of high-energy protons in the backward direction is improbable, only a low flux of suitable protons was obtained. The detected positive pions were also emitted in the backward direction, while the negative pions were emitted in the forward direction. The π^+/π^- ratio in a given direction usually considerably exceeds 1, but with this experimental arrangement and for this low meson energy, the ratio was near unity.

Before an exposure, the magnetic field was stabilized by permitting the cyclotron magnet to warm up for several hours. During an experiment the current was maintained at a standard value; a potentiometer was used to monitor it. Fluctuations of about one part in 1000 were experienced.

D. Microscope Work

The exposed plates were developed and examined under high-power microscopes, magnification about 1200, using oil-immersion objectives. The long axis of the plate (the x-axis) was aligned with the lateral motion of the microscope stage by lining up the centers of the fiducial marks. The coordinates, on the microscope stage, of the fiducial centers were recorded and the plates were scanned for the tracks of the desired particles. When these were found the coordinates of the first developed grain in the track were taken as the point of entry. The microscope stages used enabled one to read the x and y coordinates of a point to one micron, but because the fiducial lines were somewhat diffuse and about 20 microns in width, the

absolute location of a point was known only to about 10 microns. Emulsion distortion also contributed to this uncertainty. The angle θ of the track with respect to a local y axis through the point of entry was measured with an eyepiece goniometer. The standard error of the angle measurement was about 1°. This uncertainty was caused largely by the scattering of the particle in the emulsion. The range of the particle was measured by recording the lengths of successive straight segments of track as measured either on a calibrated eyepiece reticle or by the stage coordinates. The distance between the beginning and end of each segment of track was measured. A correction was applied to the depth measurement for the shrinkage. The total range was corrected 0.9 micron for the finite grain spacing.[20]

Three observers took data. One measured tracks by means of the eyepiece reticle, the other two used the stage coordinates. Great care was taken to insure that all three were using comparable standards. Many cross checks were made: One observer measured a track using his microscope and method and then the plate was given to another observer who used his technique to measure the same track. In all cases the difference found was of the same order as the error in measurement for a single observer (about $0.1 \times R^{1/2}$ microns). Since any one observer measured all ranges by the same method, an absolute calibration of his range scale was not necessary for finding the ratio of the masses nor for determining the absolute momentum, since only range ratios are required. The dip angle δ was also recorded. Although the measurement of this quantity offers some difficulties because of particle scattering and emulsion shrinkage, it was measured with a standard deviation of about 1°. On the basis of abnormal dip angle measurements, some tracks were not measured in Experiment 3, but Experiments 1 and 2 were remarkably free of stray particles. This is illustrated by Fig. 8, which shows the distribution of normalized ranges of all the positive pions found in Experiment 2.

The measured average dip angle, when compared with that derived from the dimensions of the apparatus, provides an over-all check of the geometry, shrinkage factor, and the z-axis calibration of the microscope.

E. Magnetic Measurements

Absolute measurements of the magnetic field were carried out by use of a Varian Associates Nuclear Induction Fluxmeter. In the preliminary experiments, the proton-moment head, containing the water sample and coils, was mounted directly on top of the channel, and the Larmor frequency was measured at the same time as the plate was exposed. This arrangement proved very cumbersome for efficient operation. The preliminary measurements showed that the magnetic field intensity (for the same excitation current) on different days remained constant to within a few gauss. This is not particularly surprising, as the magnet operated near saturation. A simpler procedure could therefore be adopted. After the plate exposures were completed, the field measurements were made within a few hours. The magnet excitation current was kept constant during this period by means of a Leeds and Northrup potentiometer. The proton-moment head was inserted into the cyclotron by means of a special probe. The measurements were made in vacuum. In addition to measurements along a radial line, measurements were made along the proton orbit, and along the mirror image of the proton orbit. It was found that the radial behavior of the field along the proton orbit was the same as that along the Central Radial Line, but an azimuthal variation of up to 0.1% was found on the mirror-image orbit. This perturbation was probably caused by the proximity of the vacuum tank wall. The azimuthal effect was too small to measure when the positive and negative pion orbits were compared.

Measurements of the absolute field intensity as a function of cyclotron radius were made many times in the period 1950-53. After the magnet

current had been set for 5 or 6 hours, the individual values obtained all fell within ± 0.1 percent of the mean value even when the measurements were repeated on widely different dates. The Larmor frequency, and therefore the value of the field, was read with about 0.03 percent error for any one determination.

VIII. RESULTS

A. Positive Pion/Proton Mass Ratio

The six plates of Experiments 1 and 2 each yielded values for this ratio. Corrections were made for (a) the finite size of target and detector, (b) the Lewis Effect, and (c) the emulsion distortion. To illustrate the magnitudes of the corrections, they are itemized in Table III along with the mass ratios found. It may be seen that the corrections are small, but not quite negligible. We obtain the weighted mean result

$$m_{\pi^+}/m_p = 0.14887 \pm 0.00011 .$$

The error indicated is the probable error. The chief contribution to the uncertainty, here as in the subsequent experiments, arose from the inherent Bohr straggling in the ranges. As seen in Figs. 7 and 8, the Rp^{-q} have the expected normal distributions, and Table II lists the sources of variance.

The internal-external consistency[25] is good, since the ratio of the two errors is unity.

If the proton mass is taken equal to 1836.1 electron masses,[26] then the mass of the positive pion in units of the electron mass is

$$m_{\pi^+} = 273.3 \pm 0.2 .$$

Table III

Positive pion/proton mass ratio determinations with corrections for systematic effects. ΔR and $\Delta R'$ are the respective extensions of pion and proton ranges (in microns) caused by emulsion distortion.

Plate	n	n'	3.44×10^4	$'3.44 \times 10^4$	$e_1 \times 10^4$	$e_1' \times 10^4$	ΔR (μ)	$\Delta R'$ (μ)	Uncorrected mass ratio	Corrected mass ratio and prob.error
27152	56	10	4.28	1.87	7.44	1.11	-0.9	-3.2	0.14890	0.14892±0.00030
27153	49	10	-1.19	1.98	"	"	+0.1	+0.4	0.14837	0.14841±0.00027
27154	51	10	7.72	2.02	"	"	+0.3	+1.2	0.14936	0.14944±0.00029
28848	65	10	9.20	1.94	"	"	-0.4	-2.2	0.14914	0.14913±0.00024
28849	69	10	9.34	1.92	"	"	+2.0	+9.4	0.14828	0.14841±0.00027
28853	78	10	9.83	1.90	"	"	+1.7	-19.6	0.14858	0.14891±0.00025

Weighted mean = 0.14887

Probable error (internal consistency) ±0.00011

Probable error (external consistency) ±0.00011

B. Negative Pion/Positive Pion Mass Ratio

Three plates studied in Experiment 1 yielded data for the calculation of this ratio. Since the particles came from the target during the same bombardment interval and the apparatus was symmetrical for reception of the two types, a number of sources of error were eliminated. Geometrical factors were excluded and the only significant corrections were (a) the difference in stopping power for positive and negative particles, and (b) the emulsion distortion. Table IV lists the mass ratios determined in the individual plates and the final weighted mean corrected for the difference in stopping

power of the positive and negative pions in emulsion. (Section IV-B.) The final result obtained is

$$m_{\pi^-}/m_{\pi^+} = 0.998 \pm 0.002 .$$

We may also compute the negative pion mass directly from the π^-/proton mass-ratio observed in Experiment 1. Making all corrections, we obtain in electron-mass units

$$m_{\pi^-} = 272.8 \pm 0.3 .$$

Table IV

Negative pion/positive pion mass ratio determinations

Plate	n	n'	Uncorrected mass ratio	Mass ratio corrected for distortion
27152	54	56	0.9908	0.9919 ± 0.0021
27153	49	49	0.9993	0.9992 ± 0.0023
27154	44	51	1.0009	1.0006 ± 0.0023

Weighted mean = 0.9969

(with Fermi correction for stopping difference) = 0.9979

Probable error (internal consistency) = ± 0.0014

Probable error (external consistency) = ± 0.0018

C. Positive Pion/Positive Muon Mass Ratio

In Experiment 3 the data were obtained from five plates. Corrections have been made for the Lewis Effect and for the finite target and detector dimensions. Since the emulsion peeled off the glass backing, adequate distortion measurements were not completed. Fortunately this ratio is very insensitive to the distortion, since the pions and muons enter the emulsion from the same direction with residual ranges differing only by about 30%.

Furthermore, the distortion effect varies in sign and magnitude from plate to plate, so that it can be treated as a random variable of mean value zero. The mass ratio, uncorrected for distortion, has been calculated for each of the five plates and a weighted mean obtained. These figures are given in Table V. We have derived the uncertainty in the mass ratio from the external consistency of the results. It is quoted as a probable error in the following:

$$m_{\pi}^{+}/m_{\mu}^{+} = 1.321 \pm 0.002 .$$

It is of interest to note in Table V that the statistical probable error as calculated from internal consistency is essentially equal to that derived from external consistency, indicating that no large systematic errors are present.

If we employ this pion-muon mass ratio with the measured positive pion mass of Sec. VIII-A, we have $m_{\mu}^{+} = 206.9 \pm 0.4$ in units of the electron mass.

Table V

Measurements of ratio of masses of positive pions to masses of positive muons

Plate	n_{π}	n_{μ}	Uncorrected mass ratio	Corrected mass ratio
25957	31	27	1.326_4	$1.325_8 \pm 0.004_9$
25958	49	46	1.325_3	$1.326_5 \pm 0.003_6$
25959	50	38	1.322_7	$1.320_5 \pm 0.003_8$
25961	51	30	1.321_3	$1.322_0 \pm 0.003_6$
25967	52	20	1.311_0	$1.307_9 \pm 0.004_3$

n_{π} and n_{μ} are the respective numbers of pions and muons measured on each plate

Weighted mean = 1.321 ± 0.002

Probable error (internal consistency) = $\pm 0.001_7$

Probable error (external consistency) = $\pm 0.002_0$

D. The Absolute Muon Decay Momentum

Experiments 2 and 3 each yield data from which to calculate the center-of-mass momentum, p_o, acquired by the muon when the pion decays. The information is summarized in Table VI. The finite target-detector corrections were again made in both experiments. The Lewis Effect was corrected for in Experiment 2 (see Eq. (33)). In Experiment 3, however, the Lewis Effect correction vanishes as muons are compared with muons (see Eq. (31)). In neither case was a correction made for emulsion distortion. The argument here is the same as in the determination of the pi/mu mass ratio. The ratio of the internal to external probable errors is again equal to unity within the statistics of the experiment. The final probable error quoted below is calculated from the external consistency of the data. Since the determination of a final mean value for p_o from both runs involves interrelated and dependent quantities, a simple averaging of the two values is not valid. The process of deriving the most probable value for p_o and its error is rather too detailed for presentation here, but is treated in Reference 21. We quote:

$$p_o = 29.80 \pm 0.04 \text{ Mev/c} .$$

Table VI

Summary of absolute decay momentum measurements

Experiment	Plate	Uncorrected momentum (10^{-5} gauss-mm)	Corrected momentum (10^{-5} gauss-mm)	Statistical[a] probable error (10^{-5} gauss-mm)
	28848	9.947	9.948	± 0.016
2	28849	9.913	9.912	± 0.018
	28853	9.924	9.924	± 0.018
	25957	9.946	9.954	± 0.026
	25958	9.967	9.961	± 0.020
3	25959	9.911	9.930	± 0.017
	25961	9.945	9.943	± 0.019
	25967	10.019	10.046	± 0.026

[a]Does not include uncertainty in absolute value of magnetic field

Expt. 2: Weighted mean = 9.958×10^5 gauss-mm.

Statistical probable error (internal consistency) = $\pm 0.009 \times 10^5$ gauss-mm

Statistical probable error (external consistency) = $\pm 0.011 \times 10^5$ gauss-mm

$p_{o\ 2} = 29.85 \pm 0.05$ Mev/c (including uncertainty in absolute magnetic field)

Expt. 3: Weighted mean = 9.929×10^5 gauss-mm

Statistical probable error (internal consistency) = 0.010×10^5 gauss-mm

Statistical probable error (external consistency) = 0.007×10^5 gauss-mm

$p_{o\ 3} = 29.77 \pm 0.05$ Mev/c (including uncertainty in absolute magnetic field)

E. The Mass of the Neutral Decay Particle

If we employ the method of least squares to calculate the weighted mean value for m_ν with its associated probable error, we are led to an cumbersome algebraic expression. The derived mass of the presumed neutrino is extremely sensitive to slight variations in a, p_o, and m_μ. Therefore, because of the statistical uncertainties in the values of these parameters, the exact analytical solution is not attempted and a graphical method is applied. Higher accuracy is also achieved if one replaces m_μ in Eq. (25) by the quantity m_π/a, where m_π is the value for the pion mass. The graphical solution is presented in Fig. 9. A family of curves for different values of m_ν/m_μ can be plotted as a function of a and the quantity $p_o/m_\pi c$. The hatched region is the area subtended by their probable errors. If one substitutes the final weighted means given above for these parameters into Eq. (25), one finds $(m_\nu/m_\mu)^2 = 0.0001$, but with an error of $\pm$ 0.0004. Examination of Fig. 9 indicates a probable upper limit to the mass of the neutral decay particle of 7 electron masses.

F. The Pi-Mu Mass Difference and the Mass of the Muon

As mentioned previously in Sec. VI-A, certain mass relations are insensitive to the mass of the neutral decay particle if m is small. Therefore, if we assume $m_\nu = 0$, we obtain the following results (in units of the electron mass):

Expt. 2: $m_\pi^+ - m_\mu^+ = 66.53 \pm 0.10$

Expt. 3: $m_\pi^+ - m_\mu^+ = 66.32 \pm 0.10$

Mean: $m_\pi^+ - m_\mu^+ = 66.41 \pm 0.07$

Introducing the pion value into our final weighted mean value for the π-μ mass difference, we have

$$m_\mu^+ = 206.9 \pm 0.2 .$$

This value represents the most accurate determination of the mass of the positive muon in this series of experiments.

G. The Absolute Kinetic Energy of the Muon

Assuming $m_\nu = 0$, we have, from Eq. (28),

Expt. 2: $T_o = 4.126 \pm 0.017$ Mev,

Expt. 3: $T_o = 4.117 \pm 0.023$ Mev,

Mean: $T_o = 4.123 \pm 0.016$ Mev.

The kinetic energy of the muon can also be determined from the usual relativistic energy-momentum-mass relation, Eq. (29), with no assumptions being made about the mass of the neutrino. One uses the above determinations of p_o, m_{π^+}, and the m_{π^+}/m_{μ^+} mass ratio. Here, also, the evaluation of the error in the calculation is complicated because these quantities are to some extent dependent. The complete analysis employing a graphical method once again is given in Reference 2i. One finds

$$T_o = 4.12 \pm 0.02 \text{ Mev.}$$

IX. DISCUSSION

We conclude by making some general statements regarding the philosophy of these measurements and some specific remarks about the results.

In planning a precise physical measurement it is important to anticipate the distribution of the statistics to be obtained so that spurious events (background) or excessive variance can be detected. It may be possible to construct a function of the quantity to be measured that is normally distributed with a calculable standard deviation. In such cases, all the statistical theory of the gaussian distribution is available to test the consistency of the results. In our experiments the quantity Rp^{-q} was introduced for this purpose. Measurements of this quantity had the predicted distribution; this distribution provided direct information on the statistical reliability of the data. The variance arose chiefly from the inherent straggling of ranges.

For the reduction of systematic errors, two useful principles of physical measurement are applicable. These are the ratio principle and the null principle.[27] Both have been utilized in the experiments. Only ratios of like quantities are measured, and when the equal-velocity condition is introduced, the momentum exponent q drops out of the equations and a "balance" is attained in which the ratio common to the ranges and the momenta is equal to the mass ratio. While the approach to the "null" condition can always be made by successive approximations, the initial momentum ratios we chose were already satisfactory, so that nothing was to be gained by closer matching of the velocity intervals in which the particles were selected.

It is noteworthy that the most precise indirect measurements now are in complete accord with these results. The residual difference that remains in the above-quoted positive and negative pion masses has a very low

significance level. Possibly a further study of the relative stopping powers of matter for particles of opposite sign may be justified, however.

Our analysis of the π-μ decay requires a "neutrino" to account for the missing mass-energy, momentum, and angular momentum. A fermion with momentum in Mev/c equal to its energy in Mev is required to balance the conservation relations.

The results also imply that the magnitude of the electric charge carried by mesons is identical to the electronic quantum of charge, for the apparent mass values obtained by different methods are very sensitive to the charge and depend on it in different ways.

This work stems from early experiments of E. Gardner and C. M. G. Lattes,[28] and their ideas have been retained in some of the experimental procedures. Before poor health forced the discontinuance of his work, many aspects of these experiments were planned in discussions with Dr. Gardner. Throughout the extended period during which this work was carried on, we enjoyed the invaluable cooperation of many individuals in the Radiation Laboratory. In particular, we are indebted to Mrs. T. Griswold for aid in plate measurements, to James Vale and Lloyd Houser for reliable cyclotron operations, and to the computing group, under the leadership of John Killeen, for aid in the reduction of data.

This work was done under the auspices of the U. S. Atomic Energy Commission.

REFERENCES

1. Many of the earlier measurements are reviewed in:
   (a) J. A. Wheeler and R. Ladenburg, Phys. Rev. 60, 754 (1941).
   (b) C. F. Powell, Reps. Prog. in Phys. 13, 350 (1950) (London: Physical Society).
2. The development of this mass-ratio method has been partially reported in the following:
   (a) W. H. Barkas, UCRL Memorandum, May 12, 1949.
   (b) W. H. Barkas, Proceedings of the Echo Lake Cosmic Ray Symposium, June 23, 1949.
   (c) W. H. Barkas, F. M. Smith, and E. Gardner, Phys. Rev. 82, 102 (1951).
   (d) W. Birnbaum, F. M. Smith, and W. H. Barkas, Phys. Rev. 83, 895(A) (1951).
   (e) W. H. Barkas, Am. J. Phys. 20, 5 (1952).
   (f) F. M. Smith, W. Birnbaum and W. H. Barkas, Phys. Rev. 91, 765 (1953).
   (g) W. H. Barkas, Meson Mass Measurements I - Theory of the Mass Ratio Method, University of California Radiation Laboratory Report No. UCRL-2327, (1953).
   (h) F. M. Smith, Meson Mass Measurements II - On the Measurement of the Masses of Charged Pions, University of California Radiation Laboratory Report No. UCRL-2371, (1953).
   (i) Wallace Birnbaum, Meson Mass Measurements III - The Pi-Mu Mass Ratio and Energy Balance in Pion Decay, University of California Radiation Laboratory Report No. UCRL-2503 (1954).

3. Some of the early meson mass measurements by grain count and range were made by the following: C. M. G. Lattes, G. P. S. Occhialini, and C. F. Powell, Proc. Phys. Soc. London 61, 173 (1948); L. Van Rossum, Compt. Rend. 228, 676 (1949); and J. K. Bowker, Phys. Rev. 78, 87 (1950).

4. R. B. Brode, Revs. Modern Phys. 21, 37 (1949), Phys. Rev. 75, 904 (1949); W. B. Fretter, Phys. Rev. 70, 625 (1946); J. G. Retallack and R. B. Brode, Phys. Rev. 75, 1716 (1949); T. C. Merkle, E. L. Goldwasser, and R. B. Brode, Phys. Rev. 79, 926 (1950); G. M. Nonnemaker and J. C. Street, Phys. Rev. 82, 564 (1951); C. Franzinetti, Phil. Mag. 41, 86 (1950); I. Barbour, Phys. Rev. 78, 518 (1950); G. Ascoli, Phys. Rev. 90, 1079 (1953).

5. Examples: E. J. Williams and E. Pickup, Nature 141, 648 (1938); D. R. Corson and R. B. Brode, Phys. Rev. 53, 215, 773 (1938); and J. C. Street and E. C. Stevenson, Phys. Rev. 52, 1003 (1937).

6. S. Lattimore, Nature 161, 518 (1948); and Y. Goldschmidt-Clermont, D. T. King, H. Muirhead, and D. M. Ritson, Proc. Phys. Soc. 61, 183 (1948).

7. R. B. Leighton, C. D. Anderson, and A. J. Seriff, Phys. Rev. 75, 1432 (1949); A. Lagarrigue and C. Peyron, Compt. Rend. 233, 478 (1951); J. H. Davies, W. O. Lock and H. Muirhead, Phil. Mag. 40, 1250 (1949); H. J. Bramson, A. M. Seifert, and W. W. Havens, Jr., Phys. Rev. 88, 304 (1952); R. Sagane, W. L. Gardner, and H. W. Hubbard, Phys. Rev. 82, 557 (1951); and R. Sagane et al., Phys. Rev. 95, 863 (1954).

8. V. Z. Peterson, E. Iloff, and D. Sherman, Phys. Rev. 81, 647 (1951), and W. F. Cartwright, Phys. Rev. 82, 460 (1951).

9. W. K. H. Panofsky, R. L. Aamodt, and J. Hadley, Phys. Rev. 81, 565 (1951); and K. M. Crowe, and R. H. Phillips, Phys. Rev. 96, 470 (1954).

10. M. B. Stearns et al., Phys. Rev. 97, 240 (1955); 96, 804 (1954); 95, 1353 (1954); 93, 1123 (1954);
S. Koslov et al., Phys. Rev. 95, 625 (1954); M. Camac et al., Phys. Rev. 89, 905 (1953); 88, 134 (1952);
A. D. McGuire et al., Phys. Rev. 95, 625 (1954).

11. H. A. Bethe and J. Ashkin, Part II of Experimental Nuclear Physics, edited by E. Segre, Wiley, New York, 1953.

12. Such a procedure was carefully worked out by the late Dr. Eugene Gardner.

13. J. Thibaud, Phys. Rev. 45, 781 (1934).

14. W. H. Barkas, Phys. Rev. 78, 90 (1950).

15. W. Heitler, Quantum Theory of Radiation, Oxford, 1944, p. 172.

16. L. Vigneron, J. phys. radium 14, 145 (1953).

17. C. J. Bakker and E. Segre, Phys. Rev. 81, 489 (1951).

18. Communicated in a letter dated October 8, 1953, to W. H. Barkas. Professor Fermi pointed out that the Mott Theory of Scattering (see Wentzel, Handbuch der Physik, 24, Section 1, page 708) may be applied to the scattering of negative electrons by both negative and positive mesons (in the coordinate frame in which the meson is at rest). He found in this way that the average impulse transmitted to the negative meson is less than that received by a positive meson.

19. O. Heinz, Phys. Rev. 94, 1728 (1954).

20. Walter H. Barkas, Frances M. Smith, and Wallace Birnbaum, Phys. Rev. 98, 605 (1955).

21. H. W. Lewis, Phys. Rev. 85, 20 (1952).

22. A. J. Oliver, Rev. Sci. Instr. 25, 326 (1954).

23. H. Primakoff, Phys. Rev. 84, 1255 (1951); Nakano, Nichimura, and Yamaguchi, Progr. Theoret. Phys. 6, 1028 (1951); T. Eguchi, Phys. Rev. 85, 943 (1952).

24. W. F. Fry, Phys. Rev. 91, 1930 (1952).

25. R. T. Birge, Phys. Rev. 40, 213 (1932).

26. J. M. Du Mond and E. B. Cohen, Revs. Modern Phys. 25, 691 (1953).

27. It is noted that these features are combined in the Wheatstone bridge, and make it in simplicity and elegance perhaps the most perfect example of a physical instrument.

28. E. Gardner and C. M. G. Lattes, Science 107, 270 (1948).

LEGENDS FOR FIGURES

Fig. 1. Diagram illustrating the trochoidal type of median-plane orbit followed by a charged particle in the radially decreasing magnetic field of the cyclotron. The orbit is periodically tangent to the liberation limits at radii R_1 and R_2. The quantities needed for an analysis of the orbit are labeled.

Fig. 2. Schematic diagram of a particle orbit extending from the target and terminating on the plate. The point at which the particle originated (x_1, y_1, z_1), and the point at which it is detected $(x_2, y_2, -z_o - \epsilon y_2)$, are shown. The quantity ϵ is the tangent of the angle of tilt of the plate, and the coordinate system employed is a local rectangular frame with origin at the center of the target.

Fig. 3. Basic plan view of the apparatus for Experiments 1 and 2, showing the two targets and the detector plate. The targets were not in place simultaneously during the bombardments. The surface of the emulsion was somewhat below the level of the circulating beam so that the particles entered the emulsion through the upper surface with a small angle of dip.

Fig. 4. Detailed sketches of the top and side view of the apparatus for Experiments 1 and 2 mounted on the probe cart, showing

a. The proton target.

b. The stop for defining the amount of extension of the proton target.

c. Elastic member which extends the proton target when (i) is not in contact with the lock door.

d. The pion target.

e. The positive-pion channel.

f. The negative-pion channel.

g. The proton channel.

h. Nuclear-track plate on top of the plate holder.

i. The end of the extensible rod that contacts the airlock door.

Fig. 5. Drawing of target holder for Experiments 1 and 2.

Fig. 6. Perspective view of the apparatus of Experiment 3.

Fig. 7. Normalized range distributions from one of the plates of Experiment 3. Note that the small amount of background is well separated from the main distribution. (R_1 in units of microns and p in gauss-mm.)

Fig. 8. Distributions of the normalized ranges of the positive pions in the three plates of Experiment 2.

Fig. 9. Graphical solution to estimate the neutrino mass from Eq. (6). The hatched region is the area defined by the probable errors in the π/μ mass ratio and the quantity $p_o/m_\pi c$. A probable upper limit of 6 or 7 m_o is indicated.

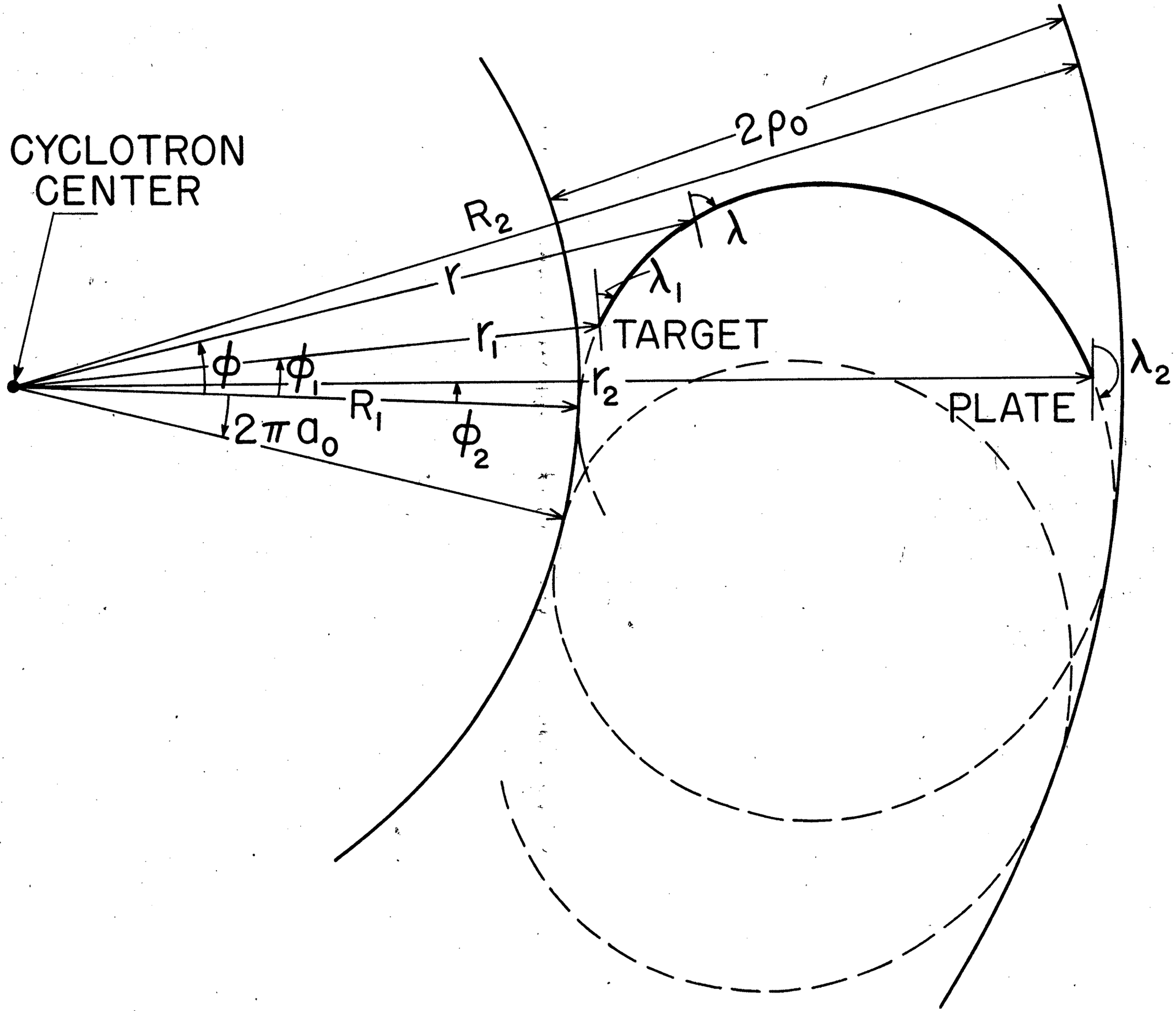
CYCLOTRON
CENTER
$2\rho_0$
R_2
r
λ
λ_1
r_1
TARGET
ϕ
ϕ_1
r_2
λ_2
R_1
PLATE
$2\pi a_0$
ϕ_2

Fig 1

14327-2

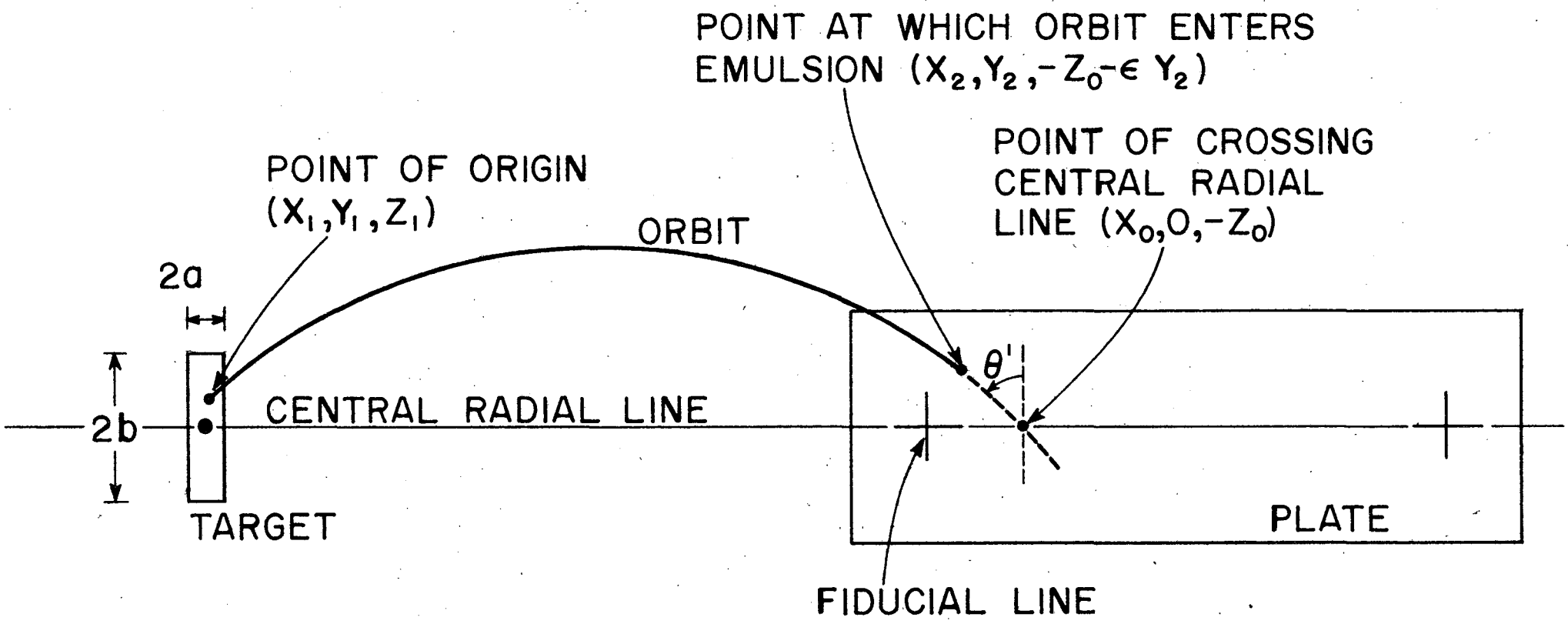
POINT AT WHICH ORBIT ENTERS EMULSION $(X_2, Y_2, -Z_0 - \epsilon Y_2)$
POINT OF CROSSING CENTRAL RADIAL LINE $(X_0, 0, -Z_0)$
POINT OF ORIGIN (X_1, Y_1, Z_1)
ORBIT
2a
2b
θ'
CENTRAL RADIAL LINE
TARGET
PLATE
FIDUCIAL LINE

Fig 2

23942-1

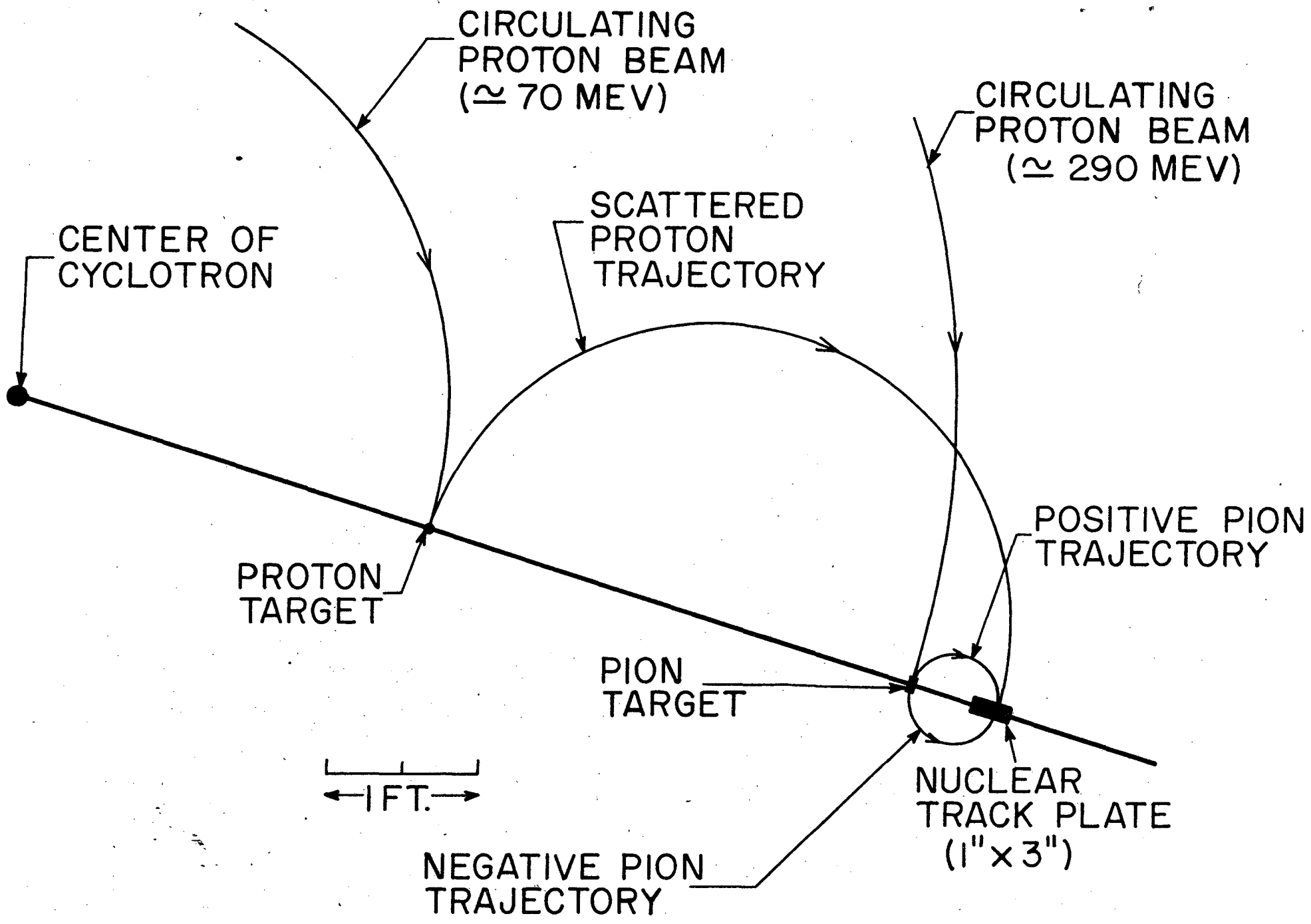
CIRCULATING
PROTON BEAM
(≃ 70 MEV)
CIRCULATING
PROTON BEAM
(≃ 290 MEV)
SCATTERED
PROTON
TRAJECTORY
CENTER OF
CYCLOTRON
POSITIVE PION
TRAJECTORY
PROTON
TARGET
PION
TARGET
1 FT.
NUCLEAR
TRACK PLATE
(1"x3")
NEGATIVE PION
TRAJECTORY

Fig 3

21978-1

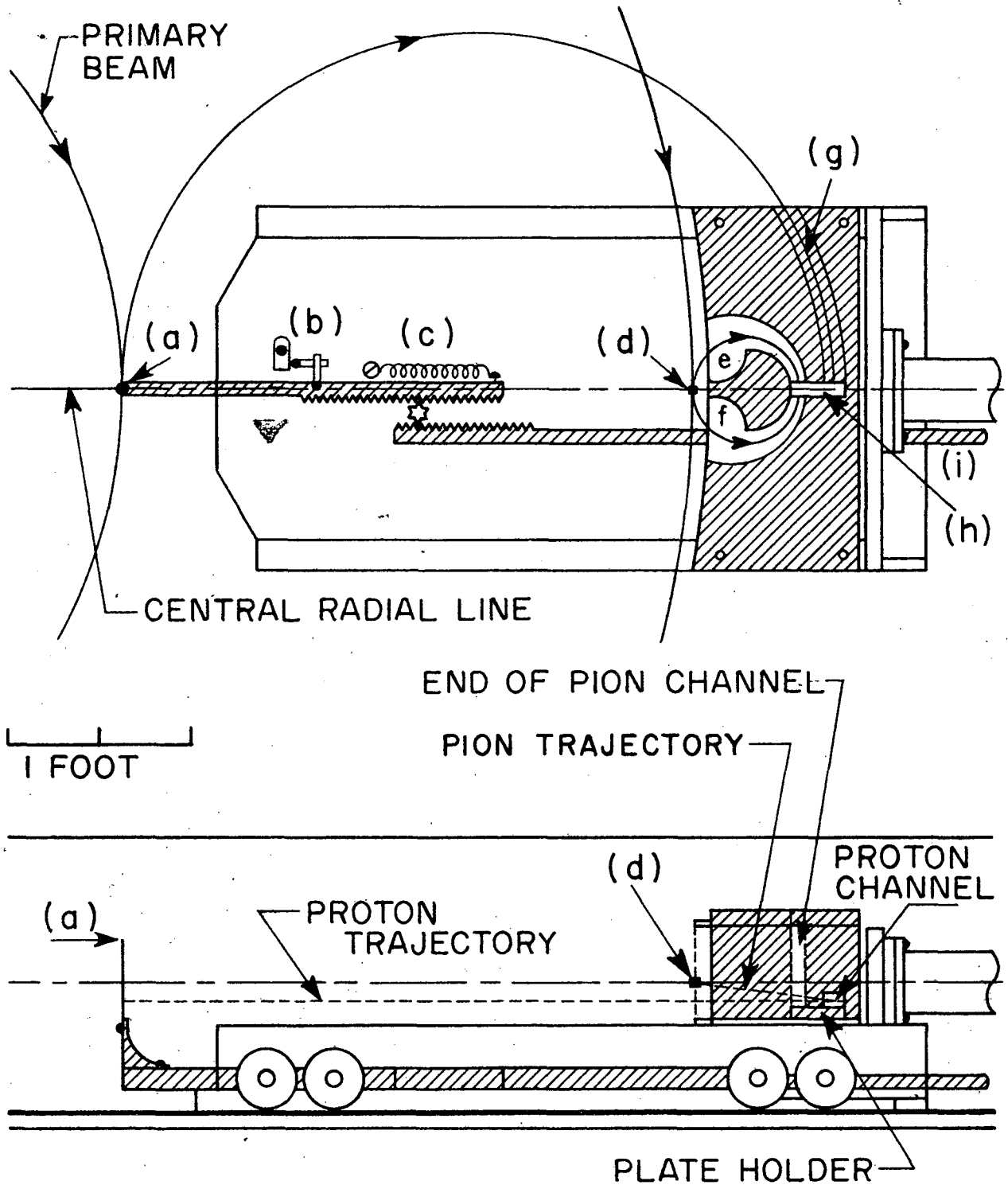
PRIMARY
BEAM
(g)
(a)
(b)
(c)
(d)
e
f
(i)
(h)
CENTRAL RADIAL LINE
END OF PION CHANNEL
PION TRAJECTORY
1 FOOT
(d)
PROTON
CHANNEL
(a)
PROTON
TRAJECTORY
PLATE HOLDER

Fig. 4

21979-1

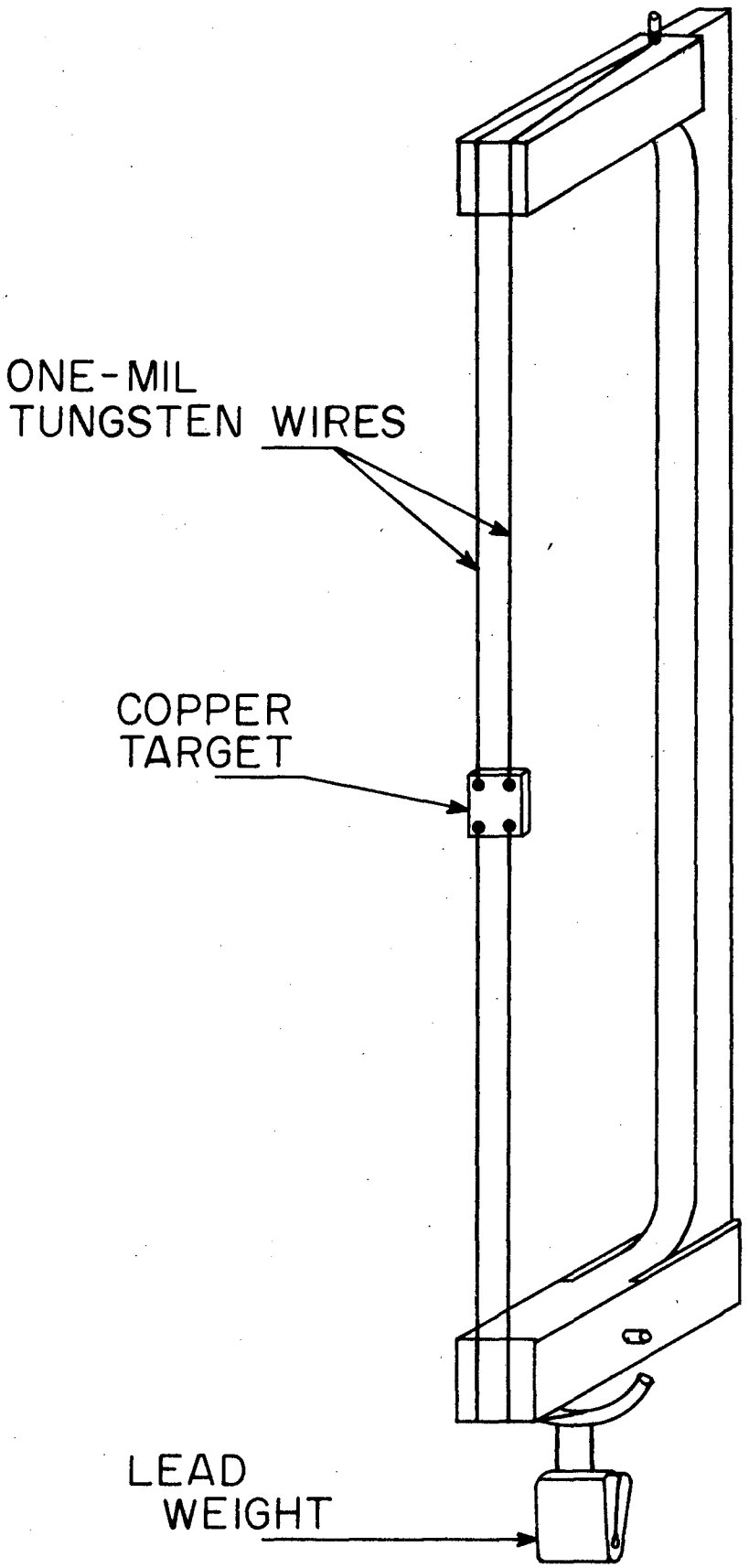

Fig 5

21727-1

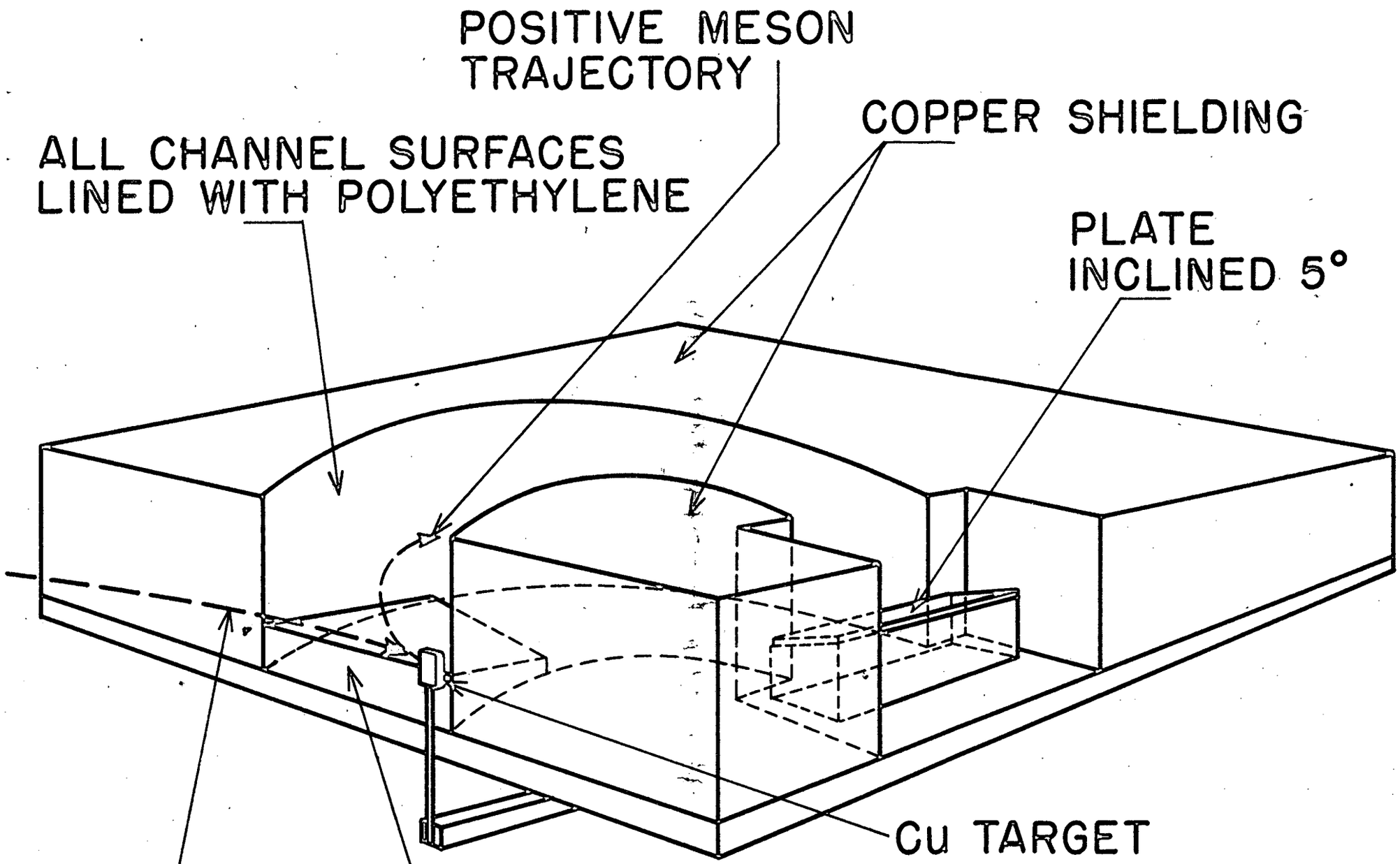
POSITIVE MESON
TRAJECTORY
COPPER SHIELDING
ALL CHANNEL SURFACES
LINED WITH POLYETHYLENE
PLATE
INCLINED 5°
Cu TARGET
CIRCULATING
PROTON BEAM
C SHADOW WEDGE ABSORBER

Fig 6

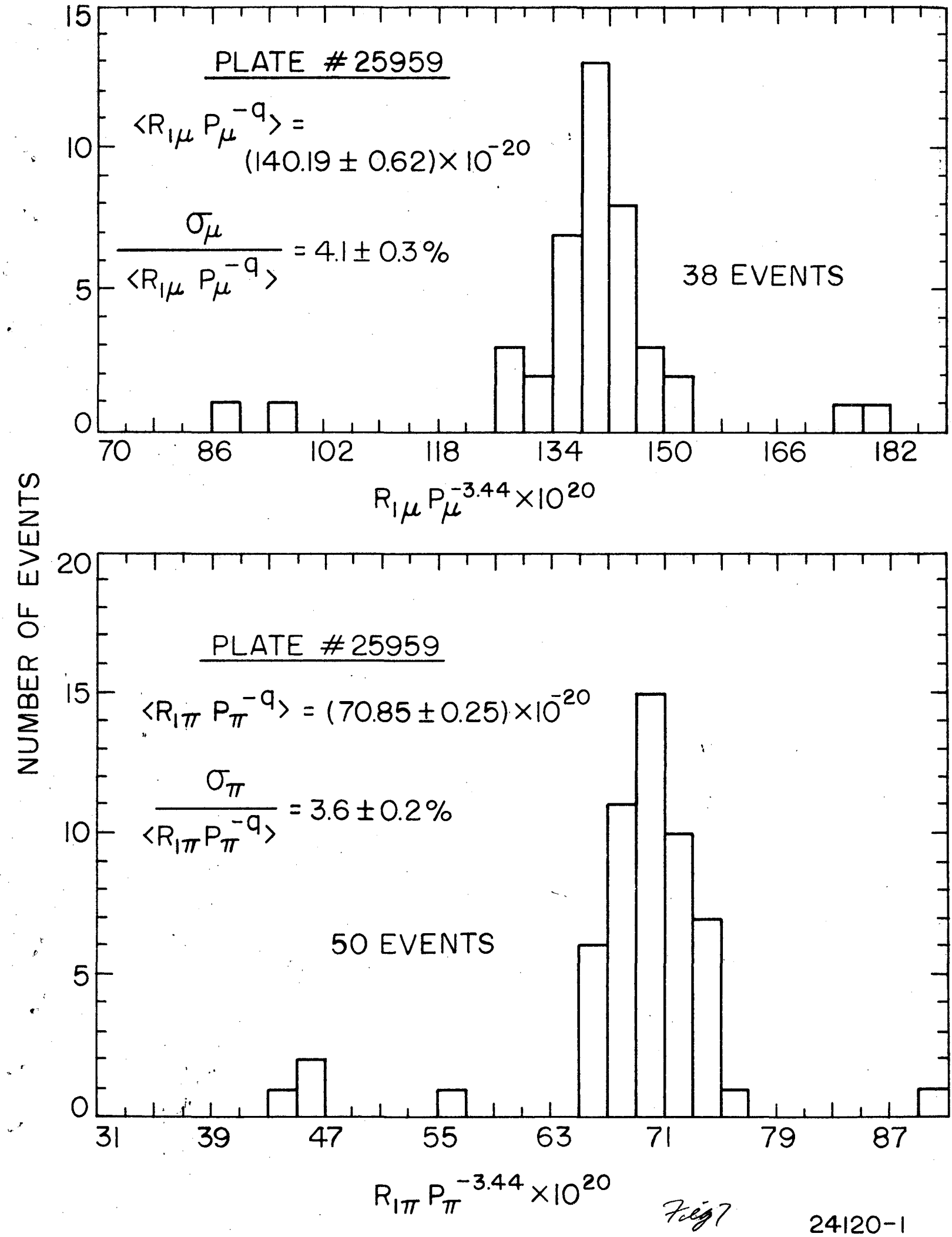
PLATE #25959
$\langle R_{1\mu} P_\mu^{-q} \rangle =$
$(140.19 \pm 0.62) \times 10^{-20}$
$\frac{\sigma_\mu}{\langle R_{1\mu} P_\mu^{-q} \rangle} = 4.1 \pm 0.3\%$
38 EVENTS
$R_{1\mu} P_\mu^{-3.44} \times 10^{20}$
PLATE #25959
$\langle R_{1\pi} P_\pi^{-q} \rangle = (70.85 \pm 0.25) \times 10^{-20}$
$\frac{\sigma_\pi}{\langle R_{1\pi} P_\pi^{-q} \rangle} = 3.6 \pm 0.2\%$
50 EVENTS
$R_{1\pi} P_\pi^{-3.44} \times 10^{20}$
NUMBER OF EVENTS

Fig 7

24120-1

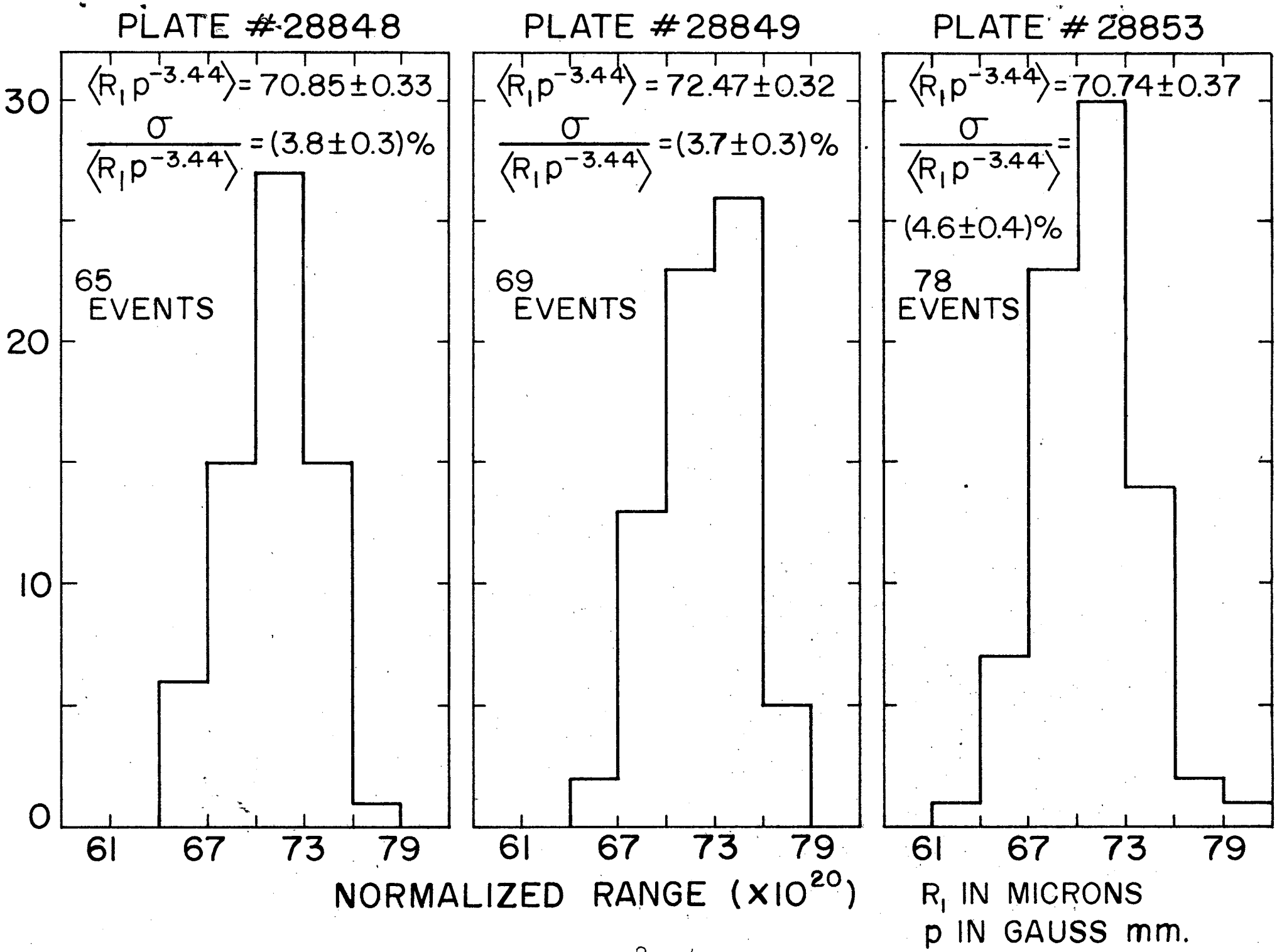
PLATE #28848
PLATE #28849
PLATE #28853
$\langle R_1 p^{-3.44} \rangle = 70.85 \pm 0.33$
$\frac{\sigma}{\langle R_1 p^{-3.44} \rangle} = (3.8 \pm 0.3)\%$
65 EVENTS
$\langle R_1 p^{-3.44} \rangle = 72.47 \pm 0.32$
$\frac{\sigma}{\langle R_1 p^{-3.44} \rangle} = (3.7 \pm 0.3)\%$
69 EVENTS
$\langle R_1 p^{-3.44} \rangle = 70.74 \pm 0.37$
$\frac{\sigma}{\langle R_1 p^{-3.44} \rangle} =$
$(4.6 \pm 0.4)\%$
78 EVENTS
30
20
10
0
61
67
73
79
NORMALIZED RANGE ($\times 10^{20}$)
R_1 IN MICRONS
p IN GAUSS mm.

Fig 4

21985-1

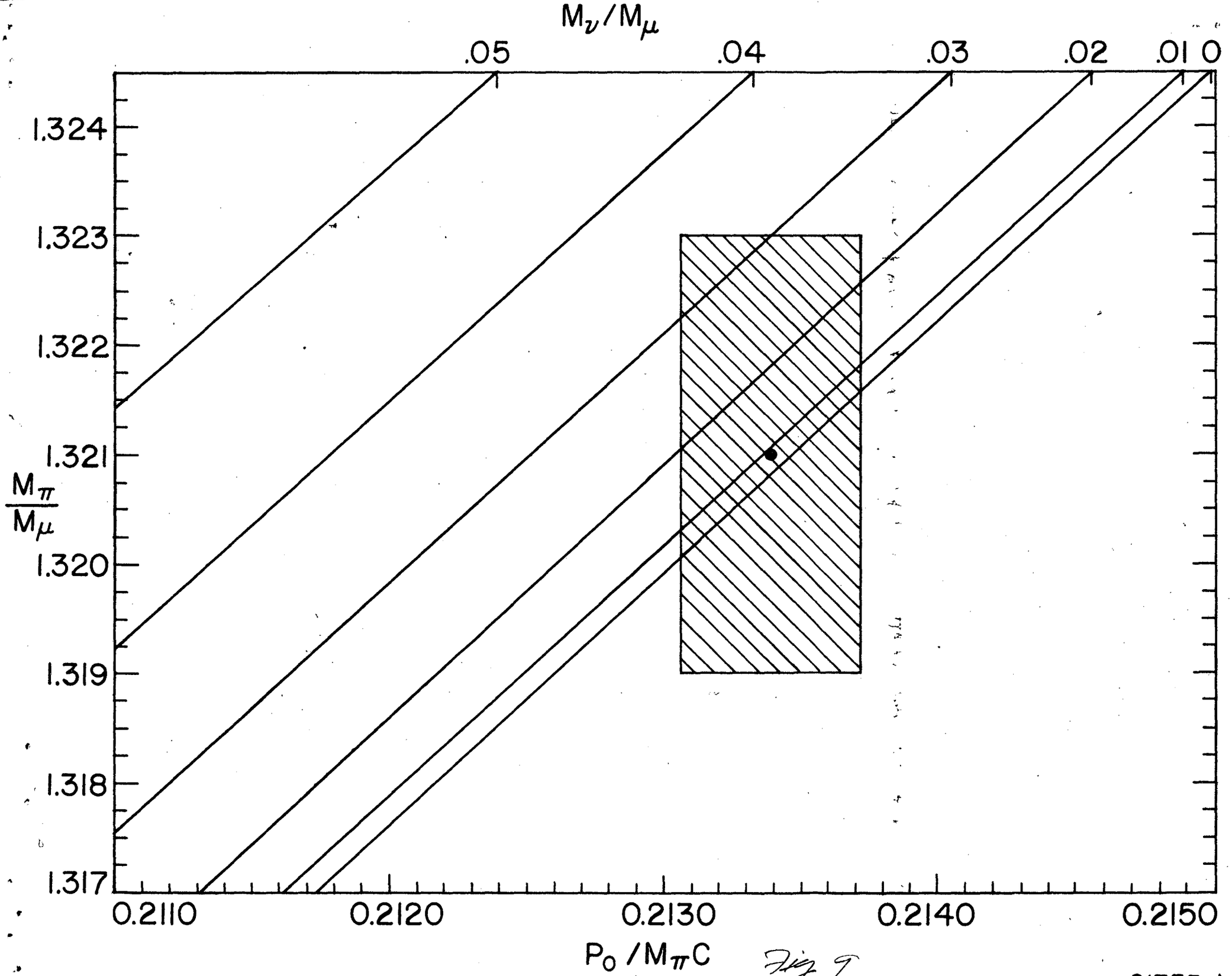
M_ν / M_μ
.05
.04
.03
.02
.01
0
1.324
1.323
1.322
1.321
1.320
1.319
1.318
1.317
$\frac{M_\pi}{M_\mu}$
0.2110
0.2120
0.2130
0.2140
0.2150
$P_0 / M_\pi C$

Fig 9

21733-1